Bovine polyomavirus-1 (*Epsilonpolyomavirus bovis*): An emerging fetal pathogen of cattle that causes renal lesions resembling polyomavirus-associated nephropathy of humans

Short title: ***Bovine polyomavirus-1* is fetopathogenic**

Federico Giannitti[1*], Caroline da Silva Silveira[1], Hannah Bullock[2], Marina Berón[1], Sofía Fernández[1], María José Benítez-Galeano[3], Nélida Rodríguez-Osorio[3], Luciana Silva-Flannery[4], Yisell Perdomo[1], Andrés Cabrera[5,6], Rodrigo Puentes[5], Rodney Colina[7], Jana M. Ritter[4], Matías Castells[7*]

[1] Plataforma de Investigación en Salud Animal, Instituto Nacional de Investigación Agropecuaria (INIA), Estación Experimental La Estanzuela, Colonia, Uruguay

[2] Synergy America Inc., Atlanta, GA, USA

[3] Unidad de Genómica y Bioinformática, Departamento de Ciencias Biológicas, Centro Universitario Regional (CENUR) Litoral Norte, Universidad de la República, Salto, Uruguay

[4] Infectious Diseases Pathology Branch, Centers for Disease Control and Prevention (CDC), Atlanta, Georgia, USA

[5] Facultad de Veterinaria, Universidad de la República, Montevideo, Uruguay

[6] Laboratorio de Interacciones Hospedero-Patógeno, Institut Pasteur de Montevideo, Montevideo, Uruguay

[7] Laboratorio de Virología Molecular, Departamento de Ciencias Biológicas, Centro Universitario Regional (CENUR) Litoral Norte, Universidad de la República (UDELAR), Salto, Uruguay

* Corresponding authors: fgiannitti@inia.org.uy (FG) and mcastells@unorte.edu.uy (MC)

Abstract

Bovine polyomavirus-1 (BoPyV-1, *Epsilonpolyomavirus bovis*) is widespread in cattle and has been detected in commercialized beef at supermarkets in the USA and Germany. BoPyV-1 has been questioned as a probable zoonotic agent with documented increase in seropositivity in people exposed to cattle. However, to date, BoPyV-1 has not been causally associated with pathology or disease in any animal species, including humans. Here we describe and illustrate pathological findings in an aborted bovine fetus naturally infected with BoPyV-1, providing evidence of its pathogenicity and probable abortigenic potential. Our results indicate that: (i) BoPyV-1 can cause severe kidney lesions in cattle, including tubulointerstitial nephritis with cytopathic changes and necrosis in tubular epithelial cells, tubular and interstitial inflammation, and interstitial fibroplasia; (ii) lesions are at least partly attributable to active viral replication in renal tubular epithelial cells, which have abundant intranuclear viral inclusions; (iii) BoPyV-1 large T (LT) antigen, resulting from early viral gene expression, can be detected in infected renal tubular epithelial cells using a monoclonal antibody raised against Simian Virus-40 polyomavirus LT antigen; and (iv) there is productive BoPyV-1 replication and virion assembly in the nuclei of renal tubular epithelial cells as demonstrated by the ultrastructural observation of abundant arrays of viral particles with typical polyomavirus morphology. Altogether, these lesions resemble the "cytopathic-inflammatory pathology pattern" proposed in the pathogenesis of *Human polyomavirus-1*-associated nephropathy in immunocompromised people and kidney allograft recipients. Additionally, we sequenced the complete genome of the BoPyV-1 infecting

the fetus, which represents the first whole genome of a BoPyV-1 from the Southern Hemisphere. Lastly, the BoPyV-1 strain infecting this fetus was isolated, causing cytopathic effect in Madin-Darby bovine kidney cells. We conclude that BoPyV-1 is pathogenic to the bovine fetus under natural circumstances. Further insights into the epidemiology, biology, clinical relevance, and zoonotic potential of BoPyV-1 are needed.

Author Summary

While bovine polyomavirus-1 seems to have a broad geographic distribution, whether this virus is responsible for disease and organ damage (lesions) in the cattle it infects is unknown. In this study, we describe and illustrate organ damage in an aborted bovine fetus naturally infected with bovine polyomavirus-1. Our results indicate that this virus is pathogenic, this means it can cause lesions and disease under natural circumstances in cattle. Interestingly, the organ damage in the fetus attributable to this viral infection closely resembles the lesions caused by related viruses within the same viral family (*Polyomaviridae*) in immunocompromised human patients and kidney transplant recipients. This study sets the bases to frame further research to learn more about whether bovine polyomavirus-1 causes abortion in cattle, and to a broader extent how polyomaviruses cause disease in animals and humans.

Introduction

Polyomaviruses are a diverse group of non-enveloped viruses with a small, circular, double-stranded DNA genome found in a wide variety of mammalian, avian, fish, amphibian, reptile, and invertebrate species [1]. As of July 2022, according to the

International Committee on Taxonomy of Viruses (ICTV, https://talk.ictvonline.org/), the *Polyomaviridae* family contained 8 genera named *Alpha*-, *Beta*-, *Delta*-, *Epsilon*-, *Eta*-, *Gamma*-, *Theta*- and *Zeta-polyomavirus*, although many strains and species are awaiting genus assignation. While some polyomaviruses can cause acute disease and even death due to productive (lytic) replication in their hosts, most of the polyomaviruses infecting mammals establish persistent subclinical infections in healthy individuals, resulting in clinical disease only after reactivation of the infection in immunosuppressed hosts [2].

Most information on the biology and medical relevance of polyomaviruses has been generated in studies of primate and murine polyomaviruses; limited information is available from other mammalian polyomaviruses in their natural hosts. Prototype diseases caused by human polyomaviruses include "polyomavirus-associated nephropathy" (PyVAN) caused by *Human polyomavirus-1* (BK polyomavirus –BKPyV–, *Betapolyomavirus hominis*) and to a lesser extent *Human polyomavirus-2* (JC polyomavirus –JCPyV–, *Betapolyomavirus secuhominis*) in kidney transplant recipients; and "progressive multifocal leukoencephalopathy" (PML) resulting from replication of JCPyV in oligodendrocytes in patients with acquired immunodeficiency syndrome or other immunomodulatory conditions [1]. Polyomaviruses have also been associated with cancer in humans and animals. For example, *Human polyomavirus-5* (Merkel cell polyomavirus –MCPyV–, *Alphapolyomavirus quintihominis*) causes Merkel cell (neuroendocrine) carcinoma of the skin [3], while *Procyon lotor polyomavirus-1* (syn. *Raccoon polyomavirus-1* –RacPyV-1–, *Alphapolyomavirus procyonis*) has been associated with tumors of the olfactory tract and brain in raccoons [4,5,6].

The polyomaviruses currently known as bovine polyomavirus (BoPyV) were initially discovered in uninoculated cultures of kidney cell lines of stump-tailed macaques, rhesus monkeys, and cynomolgus macaques, and were referred to as Stump-Tailed Macaque Virus (STMV) [7], cynomolgus kidney strain (CK-strain) of STMV [8], and Fetal Rhesus Kidney Virus (FRKV) [9]. Because of their growth in uninoculated cell cultures, it was initially thought that they were endogenous viruses of non-human primates. However, it has since been determined that they were polyomaviruses of bovine origin contaminating the bovine fetal serum used to supplement cell growth media [10]. Such contamination is frequent in commercial batches of bovine fetal/calf serum [11,12,13,14,15]. The first polyomavirus isolated in a bovine kidney cell line was obtained from a healthy newborn calf [16], and was designated Wokalup Research Station Virus (WRSV). It was suggested shortly after their discovery that STMV, FRKV, and WRSV were all isolates of an identical BoPyV [17], which was later supported by viral whole-genome sequencing of the isolate obtained by Wognum et al. [18].

Species of polyomaviruses known to infect live cattle to date include *Bos taurus polyomavirus-1* (syn. *Bovine polyomavirus-1* –BoPyV-1–, *Epsilonpolyomavirus bovis*), and *Bos taurus polyomavirus-2* (syn. *Bovine polyomavirus-2* –BoPyV-2–, awaiting genus assignation). A third species named *Bovine polyomavirus-3* (BoPyV-3, awaiting genus assignation) was originally detected in ground beef samples collected at a supermarket in the USA [19]. The complete genome sequence for BoPyV-3 is deposited in GenBank (accession KM496326), but the species is not currently listed by the ICTV. To the best of our knowledge, BoPyV-1 and BoPyV-3 have never been causally associated with pathology or disease, while BoPyV-2 has been recently proposed as a probable cause of nonsuppurative encephalitis in cattle [20].

Based on a serologic study in humans, published by authors from the United Kingdom, BoPyV has been questioned as a zoonotic agent with documented increase in seropositivity in people occupationally exposed to cattle including veterinarians, farmers, abattoir workers, veterinary technical staff, and veterinary students [17]. Although these results should be interpreted with caution due to possible cross reaction of human antibodies to other polyomaviruses [21,22], the risk of zoonotic transmission of BoPyV should not be neglected and deserves further research.

Abortion is a major health problem in cattle, resulting in huge economic losses to the livestock industry worldwide. It can be caused by many infectious and non-infectious diseases. Infectious etiologies are amongst the most frequently detected causes of abortion in ruminant fetuses subjected to routine laboratory diagnostic investigation, and include a variety of protozoal, bacterial, viral, and fungal pathogens, many of which are zoonotic [2324]. Because many bovine pathogens can be transmitted transplacentally from the dam to the fetus without necessarily resulting in abortion, detecting an infectious agent in the fetus does not warrant abortion causality. However, pathogen detection coupled with identification of pathogens within lesions observed on histopathologic examination of the aborted fetus and/or placenta is a powerful indicator of causality [25]. Given the large spectrum of possible abortigenic pathogens and the relatively few veterinary diagnostic laboratories that conduct pathologic examinations with broad pathogen detection in aborted ruminants, especially in low- and middle-income countries, it is generally accepted that known causes of abortion are underreported and that many abortifacients remain to be discovered.

The aim of this study was to describe and illustrate pathological findings in an aborted bovine fetus naturally infected with BoPyV-1, providing strong evidence to consider it fetopathogenic and a probable cause of abortion in cattle. We also sequenced

the complete genome of the involved BoPyV-1, which, to the best of our knowledge, represents the first sequence of a BoPyV-1 from the Southern Hemisphere.

Results

Case history

In March 2021, a second-gestation Holstein cow from a *Brucella*-free dairy farm in Colonia, Uruguay, aborted a male fetus at 234 days (~7.7 months) of gestation. The fetus was submitted to the veterinary laboratory of the "Instituto Nacional de Investigación Agropecuaria" (INIA) for pathologic examination.

Gross pathologic examination

At autopsy, the fetus was in good state of postmortem preservation, had a fully developed hair coat, and a crown-to-rump length of 65 cm. There was mild clear subcutaneous edema in the ventral aspect of the cervical region, diffuse petechiae in the thymus, and paintbrush hemorrhages in the serosa/adventitia of the intra-abdominal segments of the umbilical arteries, suggesting that the fetus was alive until shortly before expulsion. A moderate amount of red-tinged serous fluid was present in the abdominal, thoracic, and pericardial cavities.

Scattered throughout both kidneys there were numerous discrete pinpoint red foci with a widespread distribution alternating with areas of pallor that were visible from the capsular surface (Fig 1A), which on cut section corresponded with enhanced cortical and medullary rays in the renal parenchyma. The liver had multifocally extensive areas of roughness and white pale discoloration visible from the

diaphragmatic capsular surface. On cut section, the underlying hepatic parenchyma had increased consistency and enhanced reticular pattern characterized by numerous pinpoint pale grayish foci and interconnected linear streaks with poorly distinct borders of approximately 1 mm width alternating with reddish-orange areas of the hepatic parenchyma, resembling the so-called "nutmeg liver" (Fig 2A).

Histopathology and immunohistochemistry

The most striking microscopic lesions were in the kidneys and included severe widespread tubulointerstitial nephritis affecting predominantly the renal cortex but also the medulla (Fig 1B-D). Affected tubules were variably ectatic, frequently contained necrotic eosinophilic cellular debris sloughed into their lumens and were lined by attenuated epithelium. Multifocally, tubular epithelial cells showed either tumefaction with swollen and vesicular nuclei frequently containing one or several round or pleomorphic basophilic viral inclusion bodies, or were shrunken with angular cell borders, hypereosinophilic cytoplasm, and pyknotic nucleus or karyorrhectic debris. In affected areas, the interstitium was multifocally infiltrated by large numbers of lymphocytes, histiocytes, plasma cells, and rare neutrophils, or expanded by spindle cells with an elongate nucleus (fibroblasts) embedded in an eosinophilic fibrillar collagenous extracellular matrix, consistent with fibroplasia.

In the liver, the histoarchitecture was distorted, the hepatic cords were multifocally disorganized and separated by interconnecting bands of connective tissue (dissecting fibrosis), which also mildly expanded the portal tracts and surrounded some centrilobular veins. There was multifocal random lymphocytic and histiocytic hepatitis

with rare neutrophils, multifocal individual hepatocellular death (necrosis or apoptosis), and multifocal mild to moderate portal hepatitis (Fig 2B-D).

Other less severe lesions included mild multifocal infrequent gliosis in the brain with rare perivascular and leptomeningeal lymphocytic infiltrates, and mild megakaryocyte hyperplasia (suggestive of extramedullary hematopoiesis) in the spleen. No significant lesions were observed in the other examined tissues (see the Materials and Methods section for a list of examined tissues).

Based on the abundance of intranuclear viral inclusion bodies in the kidney, and the presence of severe histologic lesions in the liver, these two tissues were selected to perform immunohistochemical assays. The assay using a mouse monoclonal antibody raised against Simian Virus-40 (SV-40, *Macaca mulatta polyomavirus-1*, *Betapolyomavirus macacae*) large tumor (LT) antigen revealed abundant strong granular immunoreactivity in the kidney that was largely restricted to the renal tubules in both the cortex and medulla and was more intense in the nuclei of the epithelial cells (Fig 1E-F). No polyomavirus antigen was detected in a section of liver. The immunohistochemical assays for the detection of herpesviruses and adenoviruses were negative in the kidney and liver.

Transmission electron microscopy

Transmission electron microscopy evaluation revealed abundant electron-dense viral particles morphologically consistent with polyomavirus in the nuclei of renal tubular epithelial cells (Fig 3). Viral particles measuring between 35 and 43 nm in diameter were arranged in icosahedral arrays, creating inclusions within the nuclei.

Molecular virology and ancillary testing for specific pathogens

The polyomavirus VP1 fragment was successfully amplified from kidney, liver, and brain tissues by real-time polymerase chain reaction (PCR) with Ct values of 6.3, 14.8, and 19.9, respectively. Furthermore, a VP1 gene partial sequence (527 bp), amplified by conventional PCR and sequenced, confirmed the presence of BoPyV-1. PCRs for bovine herpesvirus-1, -4, and -5, and for bovine viral diarrhea virus (*Pestivirus*) were all negative. PCR for *Neospora caninum* was positive in the brain and negative in the kidney and liver. Real-time PCR for pathogenic *Leptospira* spp. was negative in the kidney and liver.

Whole genome sequencing and genome characterization

The complete BoPyV-1 genome assembly obtained in this work consisted of 4,697 bp and was assembled from 4,712 Oxford Nanopore Technology long reads with an average length of 1,248 bp and 1,090X coverage (S1 Fig). The complete genome sequence, named BoPyV-1/Faber/2021/Uy, was deposited in GenBank with accession number OM938033. The nucleotide composition was 28.7%, 21.2%, 29.9%, and 20.1% of A, C, T, and G, respectively. The genomic organization was similar to that of other BoPyV-1 reported genomes, with an early coding region containing ORFs encoding two proteins (LT antigen and small T –ST– antigen) and a late coding region containing ORFs that encode 3 structural proteins (VP1, VP2, and VP3) and a viral agnoprotein (Fig 4).

Phylogenetic analyses

The current classification system of polyomaviruses is based on the LT antigen amino acid sequence analysis. Based on this, we classified BoPyV-1/Faber/2021/Uy within the *Epsilonpolyomavirus* genus, closely related to other BoPyV-1 which is currently named *Epsilonpolyomavirus bovis* (Fig 5A). We also performed additional analyses to deepen the phylogenetic description of this fetopathogenic strain. Based on the phylogenetic analysis using complete genomes, BoPyV-1/Faber/2021/Uy grouped with other BoPyV-1 sequences, closely related to D13942 and KM496323 strains (Fig 5B). Similar results were observed when the analyses were performed using LT antigen, ST antigen, VP1, VP2, and VP3, with nucleotide and amino acid sequences; BoPyV-1/Faber/2021/Uy was also closely related to other *Epsilonpolyomavirus bovis* (S2 Fig).

Sequence identity

At the nucleotide level (Table 1), based on the complete genome, LT antigen, ST antigen, VP1, and VP3, BoPyV-1/Faber/2021/Uy showed the highest similarity (99.3%, 99.3%, 99.7%, 99.3%, and 99.2%, respectively) to D13942, ranging between 93.6% and 99.7% to other *Epsilonpolyomavirus bovis* (BoPyV-1). In the ST antigen and VP3 genes, BoPyV-1/Faber/2021/Uy also shared the same highest similarity (99.7% and 99.2%, respectively) with KM496323. Based on the VP2 gene, BoPyV-1/Faber/2021/Uy was most similar to KU200259 (99.3%), varying between 97.0% and 99.3% from other *Epsilonpolyomavirus bovis* (BoPyV-1). The nucleotide similarity ranged between 26.5% and 55.0% to BoPyV-2, and 26.7% and 48.3% to BoPyV-3.

Table 1. Comparison between BoPyV-1/Faber/2021/Uy and members of the *Epsilonpolyomavirus bovis* (BoPyV-1), BoPyV-2, and BoPyV-3 at the nucleotide and amino acid levels.

		Epsilonpolyomavirus bovis (BoPyV-1)		BoPyV-2		BoPyV-3	
		Nucleotide	Amino acid	Nucleotide	Amino acid	Nucleotide	Amino acid
BoPyV-1/Faber/2021/Uy	Complete genome	93.6–99.3	-	40.0–41.0	-	37.6	-
	Large T antigen	93.8–99.3	94.1–99.6	36.1–37.5	30.3–31.6	48.3	36.9
	Small T antigen	99.2–99.7	98.3–99.1	26.5–28.9	15.7–17.1	26.7	18.2
	VP1	97.1–99.3	98.6–99.7	53.7–55.0	50.5–52.2	39.7	27.5
	VP2	97.0–99.3	96.8–99.7	31.0–32.1	23.7–25.1	31.8	16.4
	VP3	96.1–99.2	96.1–100	36.1–37.7	20.6–22.1	30.1	13.0

At the amino acid level (Table 1), based on the LT antigen, ST antigen, VP1, and VP2 proteins, BoPyV-1/Faber/2021/Uy was most similar (99.6%, 99.1%, 99.7% and 99.7%, respectively) to D13942, varying between 94.1% and 99.7% to other *Epsilonpolyomavirus bovis* (BoPyV-1). In the VP1 protein BoPyV-1/Faber/2021/Uy also shared the same highest similarity (99.7%) with KU170643. Based on the ST antigen and VP2 proteins, BoPyV-1/Faber/2021/Uy was equally similar (99.1% and 99.7%, respectively) to all the other *Epsilonpolyomavirus bovis* (BoPyV-1) except KU200259 and KX455485, respectively. Lastly, based on the VP3 protein, BoPyV-1/Faber/2021/Uy showed 100% similarity with the other *Epsilonpolyomavirus bovis* (BoPyV-1) except KX455485 (96.1%). The amino acid identity of BoPyV-1/Faber/2021/Uy ranged between 15.7% and 52.2% to members of the BoPyV-2, and 13.0% and 36.9% to BoPyV-3.

Virus isolation

Cytopathic effect characterized by cytoplasmic vacuolation followed by lysis of Madin-Darby bovine kidney (MDBK) cells was observed 5 days after inoculation of the kidney tissue, and 4 and 5 days after inoculation of the supernatants on the two (first and second) serial passages (Fig 6A). The real-time PCR for BoPyV-1 on aliquots of the supernatant obtained at 5-, 4- and 5-days post-inoculation was positive with Ct values of 9.6, 13.2, and 14.3, respectively, demonstrating BoPyV-1 replication. No cytopathic effect was observed at the same time points in any of the MDBK cell cultures used as negative controls (Fig 6B).

Discussion

Here we describe for the first time gross and microscopic lesions in an aborted bovine fetus infected with BoPyV-1, providing evidence of its pathogenicity under nonexperimental conditions in its natural host.

Altogether, the pathological (histological, immunohistochemical, ultrastructural) findings in the kidneys of the fetus are consistent with an active polyomavirus infection with lytic replication of the virus, production of abundant intranuclear inclusion bodies composed of dense arrays of assembled virions, and LT antigen expression in the nuclei of renal tubular epithelial cells. In addition, severe degeneration (i.e., swelling, tumefaction, attenuation) and necrosis of renal tubular epithelial cells are indicative of a cytopathic viral effect, along with a prominent inflammatory response to the infection, and interstitial fibrosis suggestive of chronic active renal damage at the time of abortion. While BoPyV-1 was isolated and detected by molecular methods as well as intralesionally by immunohistochemistry and transmission electron microscopy, other DNA viruses able to produce intranuclear inclusion bodies in epithelial cells such as

herpesviruses and adenoviruses were ruled out in this case. Although BoPyV-1 had been previously detected in aborted bovine fetuses [26], the study did not include a pathologic examination of the fetuses, and the authors considered BoPyV-1 an unlikely cause of abortion. Conversely, we provide evidence to consider that BoPyV-1 is fetopathogenic in its natural host. Elucidating whether the clinical manifestation of abortion resulted from BoPyV-1-induced pathology in the fetus needs further investigation, although based on the evidence provided herein, BoPyV-1 should be considered a probable cause of abortion in cattle.

Although the pathogenic mechanisms by which most polyomaviruses induce tissue damage are not yet fully understood, five patterns of polyomavirus-induced pathology have been proposed [27]. These include: 1)- cytopathic polyomavirus pathology pattern, 2)- cytopathic-inflammatory pathology pattern, 3)- immune-reconstitution inflammatory syndrome, 4)- autoimmune polyomavirus pathology pattern, and 5)- oncogenic polyomavirus pathology pattern. The cytopathic polyomavirus pathology pattern is characterized by uncontrolled viral replication in the infected cells without significant inflammation; PML caused by JCPyV replication in the oligodendrocytes is the prototype disease for this pattern. The cytopathic-inflammatory pathology pattern is characterized by high-level virus replication with cytopathic lysis of infected cells along with necrosis and a significant inflammatory response. PyVAN in kidney allografts is the prototype disease for this pattern [27]. The lesions in the kidneys of the aborted fetus described herein best fit with this latter pattern of polyomavirus-induced pathology.

Histologically, PyVAN in humans is characterized by varying degrees of multifocal random interstitial nephritis, tubulitis, cytopathic changes and basophilic intranuclear inclusions in renal epithelial cells, interstitial fibrosis, and tubulo-interstitial

328 atrophy, depending on the stage of disease progression [28]. Interestingly, these same
329 lesions were observed in the kidneys of the aborted fetus infected with BoPyV-1. The
330 resemblance in the type of renal lesions suggests that BoPyV-1 in cattle could
331 potentially be a natural model of PyVAN, although this possibility needs to be further
332 explored.

333 Immunohistochemistry using antibodies against SV-40 LT antigen, as in this
334 report, has been shown to cross-react with other polyomaviruses such as BKPyV and
335 JCPyV in cases of PyVAN in humans [29]. In concert with this, the antibody we used
336 cross-reacted with BoPyV-1, indicating that this test can be used for viral identification
337 in formalin-fixed paraffin-embedded bovine tissues. This is not unexpected, considering
338 that LT antigen has domains that are conserved among the polyomaviruses [1].
339 However, the LT antigen amino acid sequence identity between SV-40 and BoPyV-
340 1/Faber/2021/Uy is only 37.4% (data not shown), although the similarity within the
341 recognition sites of the antibodies (epitopes) may be higher.

342 The lesions observed in the hepatic parenchyma of the aborted fetus, including
343 hepatocellular damage (i.e., scattered individual hepatocellular necrosis/apoptosis),
344 inflammation, and fibrosis, are attributable to a chronic active infection. Although we
345 were unable to clearly identify viral inclusions histologically or viral LT antigen by
346 immunohistochemistry in the liver, real-time PCR results indicate that the viral genome
347 was present in this tissue. Not finding viral inclusions nor antigen could be due to a
348 lower limit of detection of these pathologic techniques compared to real-time PCR, or to
349 a possible multifocal patchy distribution of the virus in the hepatic parenchyma. The
350 real-time PCR Ct value found in the liver (14.8) would indicate a relatively high viral
351 load in this tissue, though much lower than the one found in the kidney (Ct = 6.3). The
352 molecular detection of the virus in the liver is consistent with the previous study from

353 Belgium, in which kidney was not tested but BoPyV-1 was detected in other fetal
354 tissues (and fluids), including liver [26]. Our results indicate that the viral load is higher
355 in the kidneys, where the virus can not only be detected by real-time PCR but also
356 visualized by routine histopathology. Whether BoPyV-1 infects and replicates in other
357 fetal tissues should be explored in future research.

358 Interestingly, histologic examination of the brain of the fetus revealed mild
359 multifocal infrequent gliosis with rare perivascular and leptomeningeal lymphocytic
360 infiltrates. These lesions were mild, infrequent, and likely incidental (sublethal). Given
361 that the fetus was coinfected with *Neospora caninum*, as determined by PCR
362 amplification of DNA of this protozoan parasite from the fetal brain, these brain lesions
363 could be attributed to *N. caninum* infection. While *N. caninum* is a common
364 abortifacient of cattle, abortions caused by this protozoan usually have typical and
365 severe lesions that include multifocal encephalic necrosis along with gliosis and/or
366 inflammation of the cerebral parenchyma, and extensive non-suppurative myocarditis
367 and/or skeletal myositis [30], which were not present in this fetus. Hence, we believe
368 that, while the mild brain lesions in the fetus could have been caused by this protozoan,
369 other lesions typically found in fetuses aborted because of *N. caninum* infection were
370 lacking. Multifocal mild cerebral gliosis and perivascular or leptomeningeal
371 inflammation in the brain is occasionally present as an incidental (sublethal) finding in
372 asymptomatic bovine neonates that are born congenitally infected with *N. caninum* or
373 non-aborted infected fetuses recovered at slaughter [30,31,32]. Interestingly, somewhat
374 similar lesions including gliosis and perivascular lymphocytic encephalitis have been
375 recently described in two adult dairy cows infected with BoPyV-2 [20]. Considering
376 that BoPyV-1 was detected in the brain of the fetus by real-time PCR, although with a
377 higher Ct (19.9) indicating a lower viral load than in the kidney and liver, the

contribution of the virus in the development of these cerebral lesions should not be disregarded. However, whether BoPyV-1 contributed to these cerebral lesions, or whether *N. caninum* contributed to the clinical presentation of abortion remains under speculation. Of note, *N. caninum* PCR was negative in the fetal kidney and liver, suggesting that this parasite did not contribute to the lesions observed in these tissues.

Generally, occurrence and progression of diseases caused by polyomaviruses in mammals seem to be largely dependent on host immunosuppression [1,2]. Whether the cow or aborted fetus in this report were immunosuppressed is unknown. There was no evidence of lymphoid depletion on histologic examination of lymphoid tissues including thymus, spleen, and lymph nodes in the aborted fetus. Bovine viral diarrhea virus (*Pestivirus*), a common immunosuppressive virus of cattle, was ruled out by reverse transcriptase PCR in the fetal tissues. Additionally, *Leptospira* spp. infection, which can also cause bovine abortion with fetal renal and hepatic lesions, was ruled out by real-time PCR in the kidney and liver.

Little information is available on the epidemiology and geographic distribution of BoPyVs. An early serologic study found that 62% of 273 cattle had antibodies against the virus [17], suggesting a relatively high seroprevalence. Based on the authors' affiliations, we speculate that the tested cattle were from the United Kingdom. Similarly, a research group from The Netherlands found antibodies to the virus in sera of 25 out of 57 cattle tested (43.9%) as well as in 6/26 (23.1%) samples of bovine colostrum [8]. A study from New Zealand found that infection is more common in bovine fetuses and calves than in adult cattle when batches of bovine serum products are analyzed [14]. Studies based on molecular detection in bovine serum, beef muscle, or ground beef in the USA, Mexico, Germany, and New Zealand found DNA of BoPyV-1, -2, and/or -3 in 2–70% of the tested samples [14,15,19,33,34]. Molecular detection of

403 BoPyV-1 and/or -2 has also been documented in cattle in Spain [35], Belgium [26], and
404 Switzerland [20]. BoPyV has also been identified as an environmental contaminant in
405 Spain [36,37], Greece, Hungary, Sweden, and Brazil [36]. The name of the initial
406 polyomavirus isolated from cattle designated WRSV suggests that this virus may have
407 been isolated in Wokalup Research Station in Australia [16]. Our report broadens the
408 current knowledge on the geographic distribution of BoPyV-1 to Uruguay. Although the
409 available information is somewhat limited, BoPyVs seem to have a broad geographic
410 distribution.

411 In this work, we sequenced the whole genome of the involved BoPyV-1, which
412 to the best of our knowledge, represents the first available genome from the Southern
413 Hemisphere. However, we note that one of the BoPyV-1 complete genomes available in
414 GenBank (D13942) lacks data on its geographic origin, information that is also missing
415 in the original publications describing this isolate and sequence by researchers from The
416 Netherlands [8,18]. The genome of all known polyomaviruses encodes at least two
417 regulatory proteins, namely LT and ST antigens, and two structural proteins, the major
418 capsid protein VP1 and the minor capsid protein VP2 [1]. A third capsid protein (VP3)
419 is encoded by most polyomaviruses. Similar to other members of the *Polyomaviridae*
420 family such as BKPyV and JCPyV, BoPyV-1 also encodes the regulatory protein
421 agnoprotein which is required for efficient viral proliferation. Accordingly, BoPyV-
422 1/Faber/2021/Uy genome encodes all the previously mentioned proteins.

423 Phylogenetic analyses revealed a close relationship of BoPyV-1/Faber/2021/Uy
424 to other BoPyV-1, particularly with the first complete genome released in GenBank
425 (D13942) [18]. This close relationship was also observed in the analyses of sequence
426 identity, in which BoPyV-1/Faber/2021/Uy showed an identity higher than 99% to
427 D13942 when comparing the complete nucleotide sequence and also at both the

nucleotide and amino acid level. It is worth mentioning a particular event that was observed in the ST antigen gene, where isolate H8 (KX455485) does not present a proper coding sequence of this gene, as observed in 55% of the reads composing the BoPyV-1/Faber/2021/Uy genome. This event is caused by a T/A substitution that generates a stop codon, which may indicate that the ST antigen is not essential for virus replication and disease. It should not be overlooked that this substitution in 55% of the reads could represent a sequencing artifact.

Despite not being an objective of this work, based on the obtained results and the latest release of the ICTV classification system by the *Polyomaviridae* Study Group, we propose to assign BoPyV-2 and BoPyV-3 in the genera and species *Alphapolyomavirus secubovis* and *Deltapolyomavirus tertibovis*, respectively.

Finally, we isolated the BoPyV-1 infecting this fetus from a frozen sample of kidney. Based on the results of the histologic and ultrastructural examinations, as well as immunohistochemistry, which indicated active viral replication in renal tubular epithelial cells, we elected to attempt virus isolation on MDBK cells as they are epithelial cells of bovine kidney origin. Surprisingly, under the conditions we described (see section on materials and methods), cytopathic effect was evident 4-5 days after inoculating the cells with either the fetal kidney that had been kept frozen for nearly 1 year, or the supernatants of the first and second passages. Concurrently, high BoPyV-1 loads were identified in the culture supernatants, as determined by the low real-time PCR Ct values. Altogether the results indicate that BoPyV-1 remains viable for long periods under freezing, as expected for a non-enveloped single stranded DNA virus, and that this strain may have a high replication capacity, considering that BoPyV-1 has been regarded as a relatively slow growing virus, requiring at least 3 to 5 weeks before *in vitro* virus replication is detected by qPCR [13,38].

We conclude that BoPyV-1 is pathogenic to the bovine fetus and thus a probable cause of abortion in cattle. Pathogenicity seems to involve cytopathic viral effects with tissue damage including necrosis, inflammation, and fibrosis, with lesions resembling PyVAN in humans. Factors of the virus and host that would determine pathology and disease development, as well as the epidemiology and transmission routes, and zoonotic potential need further investigation. *In vitro* and *in vivo* studies, including experimental infections in laboratory animals and livestock using the BoPyV-1 strain isolated from this fetus would help to better understand the biology and clinical relevance of this virus.

Materials and Methods

Histopathology and immunohistochemistry

Samples of brain, kidney, liver, heart, spleen, lung, trachea, esophagus, tongue, skeletal muscle, eyelid/conjunctiva, lymph node, adrenal gland, abomasum, forestomachs, thymus, testicle, and small and large intestines were immersion-fixed in 10% neutral buffered formalin, processed, embedded in paraffin, microtome-sectioned and stained with hematoxylin and eosin for histopathology at INIA`s veterinary laboratory. Sections were examined by a veterinary pathologist under an optical microscope (Axio Scope.A1, Carl Zeiss, Germany) coupled with a color digital camera (Axiocam 512, Carl Zeiss, Germany) commanded by the ZEN software (Carl Zeiss, Germany).

Sections of liver and kidney were processed by immunohistochemical assays for the detection of viruses known to produce intranuclear inclusion bodies in epithelial cells, including polyomavirus, herpesvirus, and adenovirus. For polyomavirus, tissues

were subjected to heat-induced epitope retrieval in citrate buffer, and a mouse monoclonal antibody raised against Simian Virus-40 (SV-40, *Macaca mulatta polyomavirus-1*, *Betapolyomavirus macacae*) LT antigen (CalBiochem®, Clone PAb416, Sigma-Aldrich) was used as primary antibody at a 1:200 dilution. Colorimetric detection of linked antibodies was performed using the Mach 4 AP Polymer kit (Biocare Medical, Concord, CA, USA) followed by the visualization with Permanent Red Chromogen (Cell Marque™, Millipore-Sigma-Aldrich, Rockling, CA, USA). Slides were counterstained with Mayer's hematoxylin (Poly Scientific, Bay Shore, NY, USA) and coverslipped with aqueous mounting medium (Polysciences, Inc.).

Two immunohistochemical assays were performed for the detection of herpesviruses. For one, antigen retrieval was accomplished by treatment with proteinase K, and a rabbit polyclonal antibody raised against human herpesvirus-1 (CDC Biological Products) that cross-reacts with human herpesvirus-2 was applied at a dilution of 1:3,000. The same revealing system as described for the SV-40 immunohistochemistry was used. The other assay was performed as previously described [39] using a primary antibody against bovine herpesvirus-1.

For adenovirus immunohistochemistry, antigen retrieval was accomplished by treatment with 0.4% pepsin and a primary antibody raised against deer adenovirus that cross-reacts with bovine adenovirus was applied. This assay was performed following a previously described procedure [40] with minor modifications (the Dako Envision + system, rather than the Biocare Farma, was used as the detection system).

For each of the immunohistochemical assays, appropriate positive and negative controls were used in parallel for quality assurance purposes and identification of nonspecific immunoreactions. The immunohistochemical assays for polyomavirus and human herpesvirus-1 were conducted at the Centers for Diseases Control and

Prevention (CDC), while the assays for bovine herpesvirus-1 and adenovirus were conducted at the California Animal Health and Food Safety laboratory (University of California, Davis).

Transmission electron microscopy

Transmission electron microscopy was conducted in formalin-fixed paraffin-embedded sections of kidney, using the on-slide embedding method [41] at the CDC. Briefly, 4 µm thick sections of tissue affixed to glass slides were deparaffinized in xylene, then rehydrated and fixed in 2.5% buffered glutaraldehyde. Samples were post fixed with 1% osmium tetroxide, *en bloc* stained with uranyl acetate, dehydrated, and embedded in Epon-Araldite resin. Epoxy resin-embedded glass slide sections were immersed in boiling hot water, removed from the slides with a razor blade, and areas of interest were glued onto EM blocks. Ultrathin sections were stained with uranyl acetate and lead citrate and examined on a Thermo Fisher/ FEI Tecnai BioTwin electron microscope.

Molecular virology and ancillary testing for specific pathogens

Nucleic acids were extracted from kidney, liver, and brain samples from the aborted bovine fetus, using the MagMAX™ CORE Nucleic Acid Purification Kit (Thermo Fisher Scientific) at INIA. The extracted nucleic acids were initially processed by PCR for the detection of bovine herpesviruses-1, -4, and -5 [42,43] and reverse-transcriptase PCR for bovine viral diarrhea virus (*Pestivirus*) [44,45] at "Universidad de la República" (UdelaR), and PCR for *Neospora caninum* [46] at INIA. DNA extracted

525 from kidney and liver was also tested by a real-time PCR assay targeting the *lipL32*
526 gene of pathogenic *Leptospira* spp. [47] at INIA.

527 For polyomavirus detection, real-time PCR targeting a 77 bp fragment of the
528 VP1 gene was performed as described elsewhere [48] at UdelaR. Briefly, 12.5 µL of
529 SensiFAST Probe No-ROX Kit (Bioline®, London, UK), 5.0 µL of nuclease-free water,
530 1.0 µL of 10 µM forward primer (QB-F1-1), 1.0 µL of 10 µM reverse primer (QB-R1-
531 1), 0.5 µL of 10 µM probe (QB-P1-2), and 5 µL of DNA were mixed in 0.2-mL PCR
532 tubes.

533 A partial VP1 gene sequence (527 bp) was amplified from the DNA by a
534 conventional PCR at UdelaR. Briefly, 12.5 µL of MangoMix™ (Bioline®, London,
535 UK), 4.5 µL of nuclease-free water, 1.0 µL of 10 µM forward primer (VP1-F), 1.0 µL
536 of 10 µM reverse primer (VP1-R), 1.0 µL of dimethyl sulfoxide, and 5 µL of cDNA
537 were mixed in 0.2-mL PCR tubes. Primers and PCR conditions were previously
538 described [14]. The PCR product was visualized in 2% agarose gel, purified using
539 PureLink™ Quick Gel Extraction kit and PCR Purification Combo Kit (Invitrogen), and
540 sequenced at Macrogen Inc. (Seoul, South Korea) with Sanger technology.

541

542 Whole-genome sequencing and genome characterization

543 For BoPyV whole-genome sequencing, conducted at UdelaR, viral genomic
544 DNA was purified from the whole genomic DNA from kidney by extracting the 4–6 kb
545 region of a 1% agarose gel. DNA purity, integrity, and concentration were assessed with
546 a Qubit device (Thermo Fisher Scientific). The sequencing library was prepared with
547 the ligation sequencing kit (SQK-LSK109) following the manufacturer's instructions
548 and directly sequenced on a FLO-MIN106 flow cell in a MinION device (Oxford

549 Nanopore Technologies®, Oxford, UK) for 24 h. High-accuracy basecalling was
550 performed with Guppy v3.6.0, and reads were trimmed and filtered with Nanofilt and
551 Nanoplot [49]. Reads with quality over 10 were used in further analyses. A host
552 filtering step was done by mapping clean reads to the *Bos taurus* reference genome
553 (GCF_002263795.1_ARS-UCD1.2_genomic.fna) using Minimap2 [50]. Unmapped
554 reads were then mapped against the BoPyV-1 reference genome (NC_001442) and the
555 consensus sequence was obtained using SAMtools [51]. The obtained complete genome
556 sequence was deposited in GenBank. Genome annotation was performed using the
557 BoPyV-1 reference genome (NC_001442).

558

559 Phylogenetic analyses

560 To classify the BoPyV, a phylogenetic tree was performed using LT antigen
561 amino acid sequences. Representative sequences of all the ICTV recognized genera, all
562 the polyomavirus sequences of bovine origin available in GenBank and other
563 *Epsilonpolyomavirus* genus sequences of non-bovine origin were used. For
564 phylogenetic analysis of the complete genome, all the complete BoPyV genomes were
565 retrieved from GenBank. Finally, all the available BoPyV sequences including LT
566 antigen, ST antigen, VP1, VP2 and VP3 were used to perform additional phylogenetic
567 trees with nucleotide and amino acid sequences, to deepen the molecular
568 characterization.

569 Multiple sequence alignments were performed with Clustal Omega provided at
570 the EMBL-EBI [52-Madeira et al., 2019]. The evolutionary model for the data and a
571 maximum-likelihood phylogenetic tree were inferred with W-IQTREE [53]. Branch
572 support was estimated with the approximate likelihood-ratio test (1,000 replicates) [54].

573

574 Sequence identity

575 The alignments for complete genomes and of each individual gene and protein
576 were used to obtain the sequence identity matrices with BioEdit version 7.2.6 [55].

577

578 Virus isolation

579 A sample of fetal kidney stored in a freezer at -20°C for nearly 1 year was
580 thawed and processed for virus isolation at UdelaR. Briefly, 20 mg of sample were
581 inoculated on MDBK cells cultured in a sterile 24-well cell culture plate (Costar™,
582 Corning Inc.) with Dulbecco's minimum essential medium supplemented with 1%
583 penicillin/streptomycin solution and 5% commercial gamma-irradiated fetal bovine
584 serum (Sigma-Aldrich, USA). Cultures were kept at 37°C in an atmosphere with 5%
585 CO_2 and observed daily under inverted microscope to search for cytopathic effect. Five
586 days post-inoculation of the kidney, 100 µL of the supernatant was inoculated onto a
587 new sterile plate with the same cell line, that was similarly cultured and observed daily
588 for cytopathic effect (first passage). A second passage was performed by inoculating
589 100 µL of the supernatant obtained at 4 days post-inoculation from the first passage into
590 a new plate that was similarly cultured and observed daily for cytopathic effect. Each
591 passage was performed in triplicates, observing a cytopathic effect in each of the
592 replicates. At the same time, uninfected cells were seeded onto wells in each of the
593 plates as control of the cell culture and reagents. Aliquots of the supernatant obtained
594 from each one of the three culture plates at 5-, 4-, and 5-days post-inoculation were
595 processed for DNA extraction and BoPyV-1 qPCR as described in the molecular
596 virology section.

Acknowledgements

We thank Eduardo Vidal and Marcelo Pla from INIA for technical assistance, and the histology department, Karen Sverlow and Aníbal G. Armién from the California Animal Health and Food Safety (CAHFS) laboratory, University of California, Davis, for performing and reading the immunohistochemistry for bovine herpesvirus-1 and adenovirus.

Disclaimer

The findings and conclusions herein are those of the authors and do not necessarily represent the official position of the Centers for Disease Control and Prevention. The mention of company names or products does not constitute endorsement by the CDC.

Funding

This work was funded by grant PL_27 N-23398 of the "Instituto Nacional de Investigación Agropecuaria" (INIA), Uruguay.

Competing interests

The authors declare that they have no competing interests regarding the publication of this manuscript.

References

1- Moens U, Krumbholz A, Ehlers B, Zell R, Johne R, Calvignac-Spencer S, et al. Biology, evolution, and medical importance of polyomaviruses: An update. Review Infect Genet Evol. 2017; 54: 18–38. doi: 10.1016/j.meegid.2017.06.011.

2- Imperiale MJ, Jiang M. Polyomavirus persistence. Annu Rev Virol. 2016; 3: 517–532. doi: 10.1146/annurev-virology-110615-042226.

3- Feng H, Shuda M, Chang Y, Moore PS. Clonal integration of a polyomavirus in human Merkel cell carcinoma. Science, 2008; 319: 1096–1100. doi: 10.1126/science.1152586.

4- Dela Cruz FN, Giannitti F, Li L, Woods LW, Del Valle L, Delwart E, et al. Novel polyomavirus associated with brain tumors in free-ranging raccoons, western United States. Emerg Infect Dis. 2013; 19: 77–84. doi: 10.3201/eid1901.121078.

5- Giannitti F, Higgins RJ, Pesavento PA, Dela Cruz F, Clifford DL, Piazza M, et al. Temporal and geographic clustering of polyomavirus-associated olfactory tumors in 10 free-ranging raccoons (*Procyon lotor*). Vet Pathol. 2014; 51: 832–845. doi: 10.1177/0300985813502817.

6- Church ME, Estrada M, Leutenegger CM, Dela Cruz FN, Pesavento PA, Woolard KD. BRD4 is associated with raccoon polyomavirus genome and mediates viral gene transcription and maintenance of a stem cell state in neuroglial tumour cells. J Gen Virol. 2016; 97: 2939–2948. doi: 10.1099/jgv.0.000594.

7- Reissig M, Kelly TJ, Daniel RW, Rangan ER, Shah KV. Identification of the stumptailed macaque virus as a new papovavirus. Infect Immun. 1976; 14: 225–231. doi: 10.1128/iai.14.1.225-231.1976.

643 8- Wognum AW, Sol CJA, van der Noordaa J, van Steenis G, Osterhaus ADME.
644 Isolation and characterization of a papovavirus from cynomolgus macaque
645 kidney cells. Virology. 1984; 134(1):254–257. doi: 10.1016/0042-
646 6822(84)90293-9.
647 9- Parry JV, Richmond JE, Gardner SD. Polyomavirus in fetal rhesus monkey
648 kidney cell lines used to grow hepatitis A virus. Lancet. 1983; 1(8331): 994. doi:
649 10.1016/s0140-6736(83)92121-9.
650 10- Parry JV, Lucas MH, Richmond JE, Gardner SD. Evidence for a bovine origin
651 of the polyomavirus detected in foetal rhesus monkey cells, FRhK-4 and -6.
652 Arch Virol. 1983; 78, 151–165. doi: 10.1007/BF01311311.
653 11- Schuurman R, van Steenis B, van Strien A, van der Noordaa J, Sol C. Frequent
654 detection of bovine polyomavirus in commercial batches of calf serum by using
655 the polymerase chain reaction. J Gen Virol. 1991; 72: 2739–2745. doi:
656 10.1099/0022-1317-72-11-2739.
657 12- van der Noordaa J, Sol CJ, Schuurman R. Bovine polyomavirus, a frequent
658 contaminant of calf sera. Dev Biol Stand. 1999; 99: 45–47. doi: 10.1016/s1045-
659 1056(05)80014-4.
660 13- Nairn C, Lovatt A, Galbraith DN. Detection of infectious bovine polyomavirus.
661 Biologicals. 2003; 31: 303–306. doi: 10.1016/j.biologicals.2003.08.005.
662 14- Wang J, Horner GW, O'Keefe JS. Detection and molecular characterisation of
663 bovine polyomavirus in bovine sera in New Zealand. N Z Vet J. 2005; 53: 26–
664 30. doi: 10.1080/00480169.2005.36465.
665 15- Paim WP, Maggioli MF, Falkenberg SM, Ramachandran A, Weber MN, Canal
666 CW, et al. Virome characterization in commercial bovine serum batches—A

667 potentially needed testing strategy for biological products. Viruses, 2021; 13:
668 2425, doi: 10.3390/v13122425.
669 16- Coackley W, Maker D, Smith VW. A possible bovine polyomavirus. Arch
670 Virol. 1980; 66: 161–166. doi: doi.org/10.1007/BF01314984.
671 17- Parry JV, Gardner SD. Human exposure to bovine polyomavirus: A zoonosis?
672 Arch Virol. 1986; 87: 287–296. doi: 10.1007/BF01315306.
673 18- Schuurman R, Sol C, van der Noordaa J. The complete nucleotide sequence of
674 bovine polyomavirus. J Gen Virol. 1990; 71: 1723–1735. doi: 10.1099/0022-
675 1317-71-8-1723.
676 19- Peretti A, FitzGerald PC, Bliskovsky V, Buck CB, Pastrana DV. Hamburger
677 polyomaviruses. J Gen Virol. 2015; 96: 833–839. doi: 10.1099/vir.0.000033.
678 20- Hierweger MM, Koch MC, Seuberlich T. Bovine polyomavirus 2 is a probable
679 cause of non-suppurative encephalitis in cattle. Pathogens. 2020; 9: 620. doi:
680 10.3390/pathogens9080620.
681 21- Moens U, Van Ghelue M, Song X, Ehlers B. Serological cross-reactivity
682 between human polyomaviruses. Rev Med Virol. 2013; 23: 250–264. doi:
683 10.1002/rmv.1747.
684 22- Viscidi RP, Clayman B. Serological cross reactivity between polyomavirus
685 capsids. Adv Exp Med Biol. 2006; 577:73–84. doi: 10.1007/0-387-32957-9_5.
686 23- Clothier K. Anderson M. Evaluation of bovine abortion cases and tissue
687 suitability for identification of infectious agents in California diagnostic
688 laboratory cases from 2007 to 2012. Theriogenology. 2016; 85: 933–938. doi:
689 10.1016/j.theriogenology.2015.11.001.

690 24- Wolf-Jäckel GA, Hansen MS, Larsen G, Holm E, Agerholm JS, Jensen TK.
691 Diagnostic studies of abortion in Danish cattle 2015-2017. Acta Vet Scand.
692 2020; 62: 1. doi: 10.1186/s13028-019-0499-4.
693 25- Dorsch MA, Cantón GJ, Driemeier D, Anderson ML, Moeller RB, Giannitti F.
694 Bacterial, protozoal and viral abortions in sheep and goats in South America: A
695 review. Small Rum Res. 2021; 205: 106547. doi:
696 10.1016/j.smallrumres.2021.106547.
697 26- Van Borm S, Rosseel T, Behaeghel I, Saulmont M, Delooz L, Petitjean T, et al.
698 Complete genome sequence of Bovine polyomavirus type 1 from aborted cattle,
699 isolated in Belgium in 2014. Genome Announc. 2016; 4: e01646-15. doi:
700 10.1128/genomeA.01646-15.
701 27- Dalianis T, Hirsch HH. Human polyomaviruses in disease and cancer. Virology.
702 2013; 437: 63–72. doi: 10.1016/j.virol.2012.12.015.
703 28- Ramos E, Drachenberg CB, Wali R, Hirsch HH. The decade of polyomavirus
704 BK-associated nephropathy: State of affairs. Transplantation. 2009; 87: 621–
705 630. doi: 10.1097/TP.0b013e318197c17d.
706 29- Costa C, Cavallo R. Polyomavirus-associated nephropathy. World J Transplant.
707 2012; 2: 84–94. doi: 10.5500/wjt.v2.i6.84.
708 30- Dubey JP, Hemphill A, Calero-Bernal R, Schares G. Neosporosis in animals. 1st
709 ed. Boca Raton: CRC Press; 2017. doi: 10.1201/9781315152561.
710 31- Venturini MC, Venturini L, Bacigalupe D, Machuca M, Echaide I, Basso W, et
711 al. *Neospora caninum* infections in bovine foetuses and dairy cows with
712 abortions in Argentina. Int J Parasitol. 1999; 29: 1705–1708. doi:
713 10.1016/s0020-7519(99)00143-5.

32- Bacigalupe D, Basso W, Caspe SG, Moré G, Lischinsky L, Gos ML, et al. *Neospora caninum* NC-6 Argentina induces fetopathy in both serologically positive and negative experimentally inoculated pregnant dams. Parasitol Res. 2013; 112: 2585–2592. doi: 10.1007/s00436-013-3424-1.

33- Gräfe D, Ehlers B, Mäde D, Ellerbroek L, Seidler T, Johne R. Detection and genome characterization of bovine polyomaviruses in beef muscle and ground beef samples from Germany. Int J Food Microbiol. 2017; 241: 168–172. doi: 10.1016/j.ijfoodmicro.2016.10.024.

34- Zhang W, Li L, Deng X, Kapusinszky B, Delwart E. What is for dinner? Viral metagenomics of US store bought beef, pork, and chicken. Virology. 2004; 468: 303–310. doi: 10.1016/j.virol.2014.08.025.

35- Ben Salem N, Pérez de Val B, Martin M, Moens U, Ehlers B. Genome sequence of Bovine polyomavirus 1 detected in a Salers cow (*Bos taurus*) from Catalonia, Spain. Genome Announc. 2016; 4: e01658-15. doi: 10.1128/genomeA.01658-15.

36- Rusiñol M, Fernandez-Cassi F, Hundesa A, Vieira C, Kern A, Eriksson I, et al. Application of human and animal viral microbial source tracking tools in fresh and marine waters from five different geographical areas. Water Res. 2014; 59: 119–129. doi: 10.1016/j.watres.2014.04.013.

37- Hundesa A, Maluquer de Motes C, Bofill-Mas S, Albinana-Gimenez N, Girones R. Identification of human and animal adenoviruses and polyomaviruses for determination of sources of fecal contamination in the environment. Appl Environ Microbiol. 2006; 72: 7886–7893. doi: 10.1128/AEM.01090-06.

737 38- Byrne P. The role of the large T antigen in the in vitro replication of BPyV. M.
738 Sc. Thesis, University of Glasgow. 2009. Available from:
739 https://theses.gla.ac.uk/576/
740 39- Rodger SM, Murray J, Underwood C, Buxton D. Microscopical and antigen
741 distribution in bovine fetal tissues and placentae following experimental
742 infection with bovine herpesvirus-1 during pregnancy. J Comp Pathol. 2007;
743 137: 94–101. doi: 10.1016/j.jcpa.2007.04.022.
744 40- Woods LW, Schumaker BA, Pesavento PA, Crossley BM, Swift PK. Adenoviral
745 hemorrhagic disease in California mule deer, 1990-2014. J Vet Diagn Invest.
746 2018; 30: 530–573. doi: 10.1177/1040638718766036.
747 41- Martines RB, Ritter JM, Matkovic E, Gary J, Bollweg BC, Bullock H, et al.
748 COVID-19 Pathology Working Group. Pathology and pathogenesis of SARS-
749 CoV-2 associated with fatal coronavirus disease, United States. Emerg Infect.
750 Dis. 2020; 26: 2005–2015. doi: 10.3201/eid2609.202095.
751 42- Ashbaugh SE, Thompson KE, Belknap EB, Schultheiss PC, Chowdhury S,
752 Collins JK. Specific detection of shedding and latency of bovine herpesvirus 1
753 and 5 using nested polymerase chain reaction. J Vet Diagn Invest. 1997; 9: 387–
754 394. doi: 10.1177/104063879700900408.
755 43- Campos FS, Franco AC, Oliveira MT, Firpo R, Strelczuk G, Fontoura FE, et al.
756 Detection of bovine herpesvirus 2 and bovine herpesvirus 4 DNA in trigeminal
757 ganglia of naturally infected cattle by polymerase chain reaction. Vet Microbiol.
758 2014; 171: 182–188. doi: 10.1016/j.vetmic.2014.03.012.
759 44- Maya L, Puentes R, Reolón E, Acuña P, Riet F, Rivero R, et al. Molecular
760 diversity of bovine viral diarrhea virus in Uruguay. Arch Virol. 2016; 161: 529–
761 535. doi: 10.1007/s00705-015-2688-4.

762 45- Vilček S, Herring AJ, Herring JA, Nettleton PF, Lowings JP, Paton DJ.
763 Pestiviruses isolated from pigs, cattle and sheep can be allocated into at least
764 three genogroups using polymerase chain reaction and restriction endonuclease
765 analysis. Arch Virol. 1994; 136: 309–323. doi: 10.1007/BF01321060.
766 46- Cabrera A, Fresia P, Berná L, Silveira C, Macías-Rioseco M, Arevalo AP, et al.
767 Isolation and molecular characterization of four novel *Neospora caninum*
768 strains. Parasitol Res. 2019; 118: 3535–3524. doi: 10.1007/s00436-019-06474-9.
769 47- Stoddard RA, Gee JE, Wilkins PP, McCaustland K, Hoffmaster AR. Detection
770 of pathogenic *Leptospira* spp. through TaqMan polymerase chain reaction
771 targeting the LipL32 gene. Diagn Microbiol Infect Dis. 2009; 64: 247–255. doi:
772 10.1016/j.diagmicrobio.2009.03.014.
773 48- Hundesa A, Bofill-Mas S, Maluquer de Motes C, Rodriguez-Manzano J, Bach
774 A, Casas M, et al. Development of a quantitative PCR assay for the quantitation
775 of bovine polyomavirus as a microbial source-tracking tool. J Virol Methods.
776 2010; 163: 385–389. doi: 10.1016/j.jviromet.2009.10.029.
777 49- De Coster W, D`Hert S, Schultz D, Cruts M, Van Broeckhoven C. NanoPack:
778 visualizing and processing long-read sequence data. Bioinformatics. 2018; 34:
779 2666–2669. doi: 10.1093/bioinformatics/bty149.
780 50- Li H. Minimap2: pairwise alignment for nucleotide sequences. Bioinformatics.
781 2018; 34: 3094–3100. doi: 10.1093/bioinformatics/bty191.
782 51- Li H, Handsaker B, Wysoker A, Fennell T, Ruan J, Homer N, et al. The
783 sequence alignment/map format and SAMtools. Bioinformatics. 2009; 25:
784 2078–2079. doi: 10.1093/bioinformatics/btp352

52- Madeira F, Park YM, Lee J, Buso N, Gur T, Madhusoondanan N, et al. The EMBL-EBI search and sequence analysis tools APIs in 2019. Nucleic Acids Res. 2019; 47(W1): W636–W641. doi: 10.1093/nar/gkz268.

53- Trifinopoulos J, Nguyen LT, von Haeseler A, Minh BQ. W-IQ-TREE: a fast online phylogenetic tool for maximum likelihood analysis. Nucleic Acids Res. 2016; 44(W1): W232–W235. doi: 10.1093/nar/gkw256.

54- Anisimova M, Gascuel O. Approximate likelihood-ratio test for branches: A fast, accurate, and powerful alternative. Syst Biol. 2006; 55: 539–552. doi: 10.1080/10635150600755453.

55- Hall TA. BioEdit: A user-friendly biological sequence alignment editor and analysis program for Windows 95/98/NT. Nucl Acids Symp Ser. 1999; 41: 95–98.

Figure captions

Fig 1. Pathological findings in the kidney of the aborted fetus. A- Grossly there are numerous discrete pinpoint red foci disseminated throughout the renal cortex that are visible through the capsular surface. B- Cortical tubules are variably ectatic, contain necrotic cellular debris and are lined by either attenuated epithelium, or epithelial cells with markedly swollen vesicular nuclei, occasionally containing one or several magenta intranuclear inclusion bodies. The cortical interstitium is infiltrated by inflammatory cells, predominantly lymphocytes and histiocytes. Hematoxylin and eosin (H&E) stain, original magnification 400X. C- Similar histologic lesions as described in B but there is also marked interstitial fibrosis. H&E stain, original magnification 400X. D- Numerous cortical tubular epithelial cells have markedly swollen nuclei containing one or several magenta intranuclear inclusion bodies surrounded by a clear halo (arrows), indicating

margination of the chromatin. H&E stain, original magnification 630X. E and F. Immunoreactivity to polyomavirus LT antigen is demonstrated by red chromogen precipitate largely in the nucleus of cortical tubular epithelial cells. Immunohistochemistry (immunoalkaline phosphatase technique) with a monoclonal primary antibody against SV-40 polyomavirus LT antigen, hematoxylin counterstain, original magnifications 200X (E) and 400X (F).

Fig 2. Pathological findings in the liver of the aborted fetus. A- Cut section of the hepatic parenchyma showing an enhanced reticular pattern characterized by numerous pinpoint pale grayish foci and interconnected linear streaks alternating with reddish-orange areas of hepatic parenchyma ("nutmeg liver"). B- The hepatic histoarchitecture is distorted and hepatic cords are disorganized and separated by areas of fibroplasia characterized by spindle cells (fibroblasts) embedded in a pale eosinophilic fibrillar (collagenous) extracellular matrix. H&E stain, original magnification 400X. C- Some hepatocytes are individualized and detached from the hepatic cords, and are shrunken, with angular cell borders, hypereosinophilic cytoplasm and pyknosis or karyorrhexis (hepatocellular necrosis/apoptosis); others have one or few clear intracytoplasmic vacuoles consistent with lipidosis. There are increased numbers of lymphocytes in the sinuses (hepatitis). H&E stain, original magnification 630X. D- A portal tract (center) is infiltrated by moderate numbers of lymphocytes and macrophages (portal hepatitis). H&E stain, original magnification 400X.

Fig 3. Transmission electron microscopy in the kidney of the aborted fetus. A- The nucleus of a tubular epithelial cell contains a dense array of viral particles forming a round inclusion (7,190X, bar= 2 μm). B- Higher magnification of A showing the array of viral particles (70,000X, bar= 200 nm).

Fig 4. Genome organization of BoPyV-1/Faber/2021/Uy (GenBank accession number OM938033). The different proteins are represented with arrows according to their location in the genome; arrow direction indicates the strand. The agnoprotein (position 220–250), VP1 (position 1,540–2,637), VP2 (position 618–1,679), and VP3 (position 981–1,679) are located on one strand and the LT antigen (joined positions 2,690–4,345, 4,423–4,502 and 4,574–4,697), and the ST antigen (joined positions 4,252–4,502 and 4,574–4,697) are located on the complementary strand. The complete genome length of BoPyV-1/Faber/2021/Uy is 4,697 base pairs.

Fig 5. Phylogenetic analyses. A- Phylogenetic tree for LT antigen amino acid sequences. Representative sequences of all ICTV recognized genera, all polyomavirus sequences of bovine origin from GenBank, and the sequence obtained in this work (in red font) were used. Sequences were aligned with ClustalW. The best substitution model (rtREV+F+I+G4) and the maximum likelihood phylogenetic tree were obtained with IQ-TREE web server. Branch support analysis was SH-aLRT branch test implemented in the IQ-TREE web server (1,000 replicates). B- Phylogenetic tree using complete genome nucleotide sequences. All polyomavirus sequences of bovine origin from GenBank and the sequence obtained in this work (in red font) were used. Sequences were aligned with ClustalW, and the best substitution model (K3Pu+F+G4) and the maximum likelihood phylogenetic tree were jointly obtained with IQ-TREE web server. Branch support analysis was SH-aLRT branch test implemented in the IQ-TREE web server (1,000 replicates).

Fig 6. BoPyV-1 isolation in MDBK cells. A- Cytopathic effect after 96 hours of incubation is characterized by cytoplasmic vacuolation and lysis with loss of the monolayer (center) in infected MDBK cells. B- In the negative control, uninfected MDBK cells form a continuous monolayer. Original magnifications 200X.

859

860 **Supporting information**

861 **S1 Fig. Coverage of the Oxford Nanopore Technology reads across the genome.** In
862 the upper panel the coverage of the reads across the reference genome (GenBank
863 accession number D13942) is shown. In the lower panel, the GC content (%) and the
864 mean GC content across the reference genome is shown.

865 **S2 Fig. Phylogenetic analyses of LT antigen, ST antigen, VP1, VP2 and VP3.** The
866 maximum likelihood trees obtained with IQ-TREE web server with nucleotide (A, C, E,
867 G, and I) and amino acid (B, D, F, H, and J) sequences are shown. All the BoPyV
868 sequences available in the database were downloaded and together with BoPyV-
869 1/Faber/2021/Uy were aligned with Clustal W. The best substitution model was jointly
870 obtained with the tree using the IQ-TREE web server. The analyses were performed
871 using LT antigen (A and B), ST antigen (C and D), VP1 (E and F), VP2 (G and H), and
872 VP3 (I and J). Some sequences are not shown in the trees because IQ-TREE discarded
873 them since they were identical to others. Branch support analysis was SH-aLRT branch
874 test implemented in the IQ-TREE web server.

875

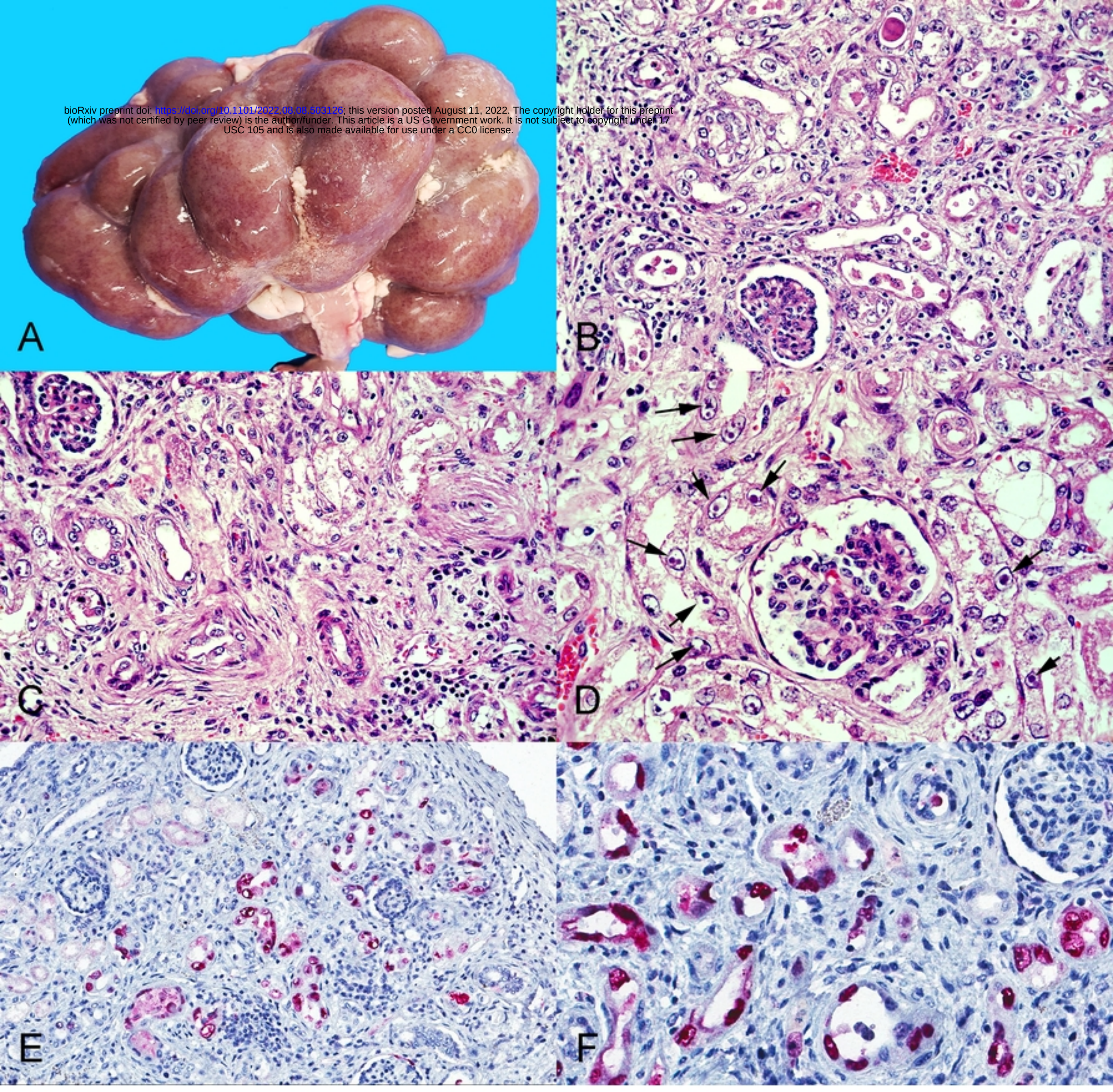

Figure

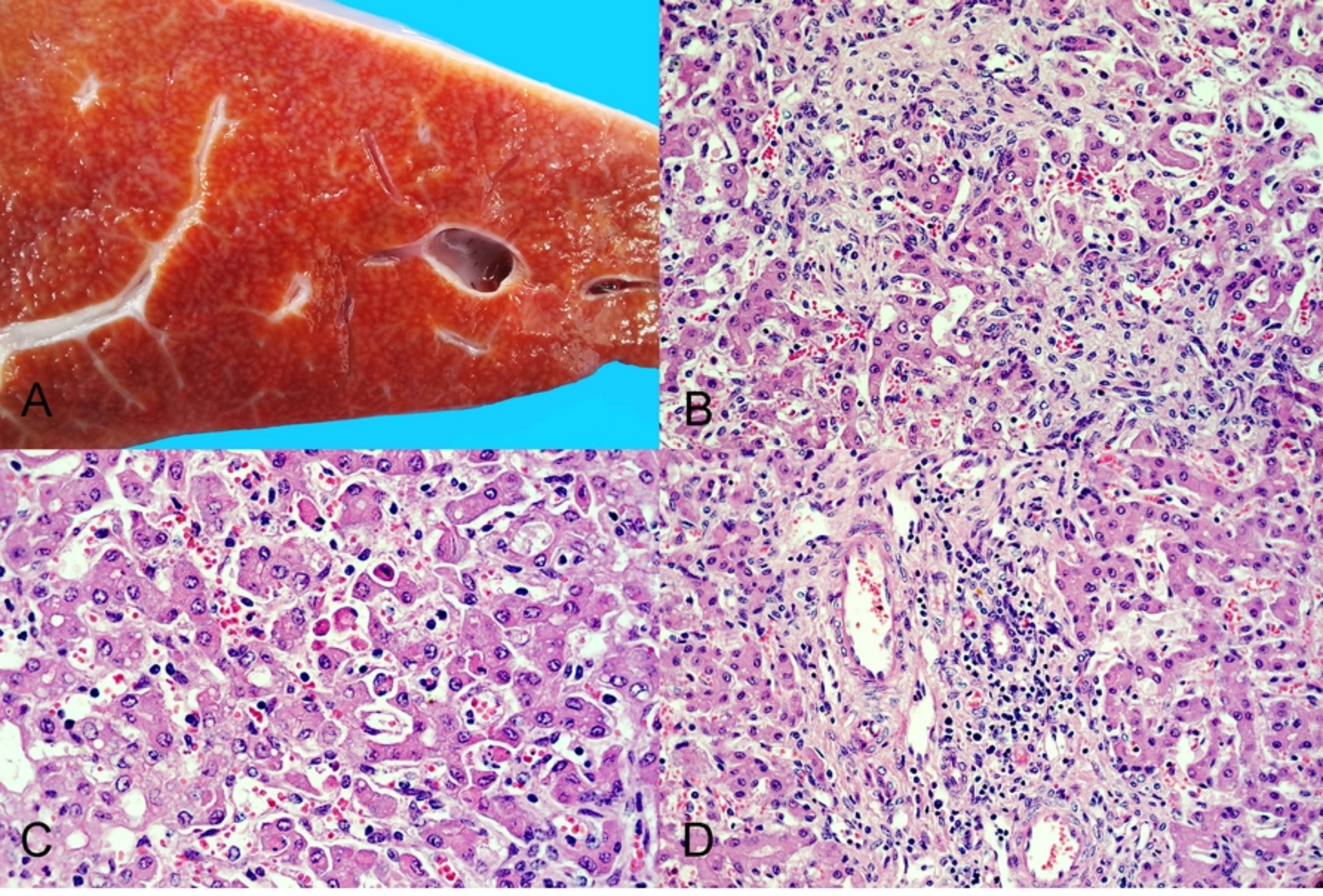

Figure

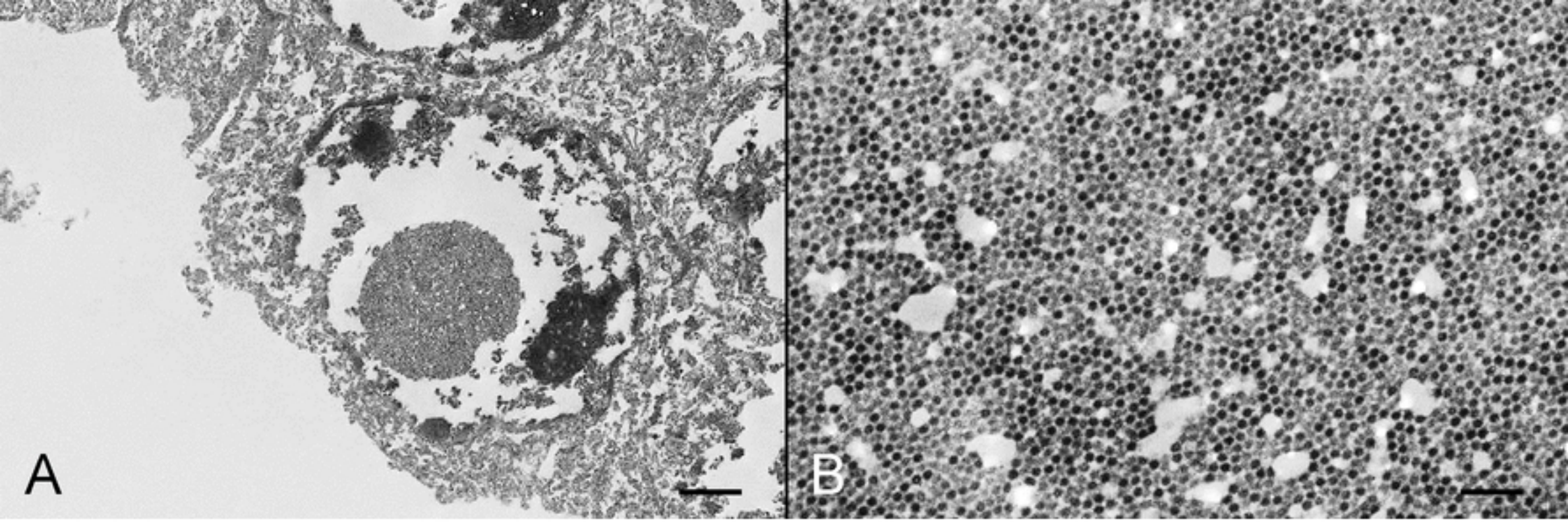

Figure

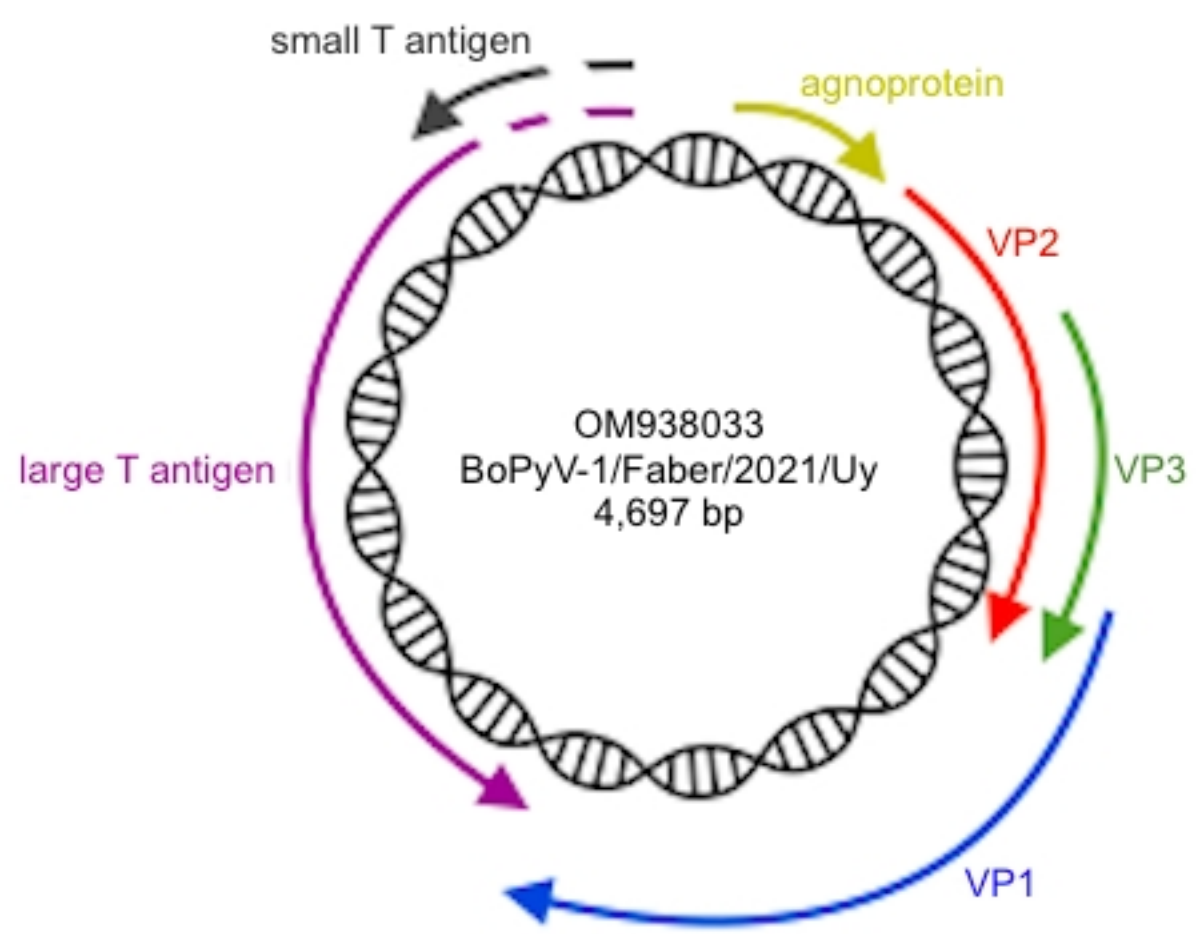
small T antigen
agnoprotein
VP2
VP3
large T antigen
OM938033
BoPyV-1/Faber/2021/Uy
4,697 bp
VP1

Figure

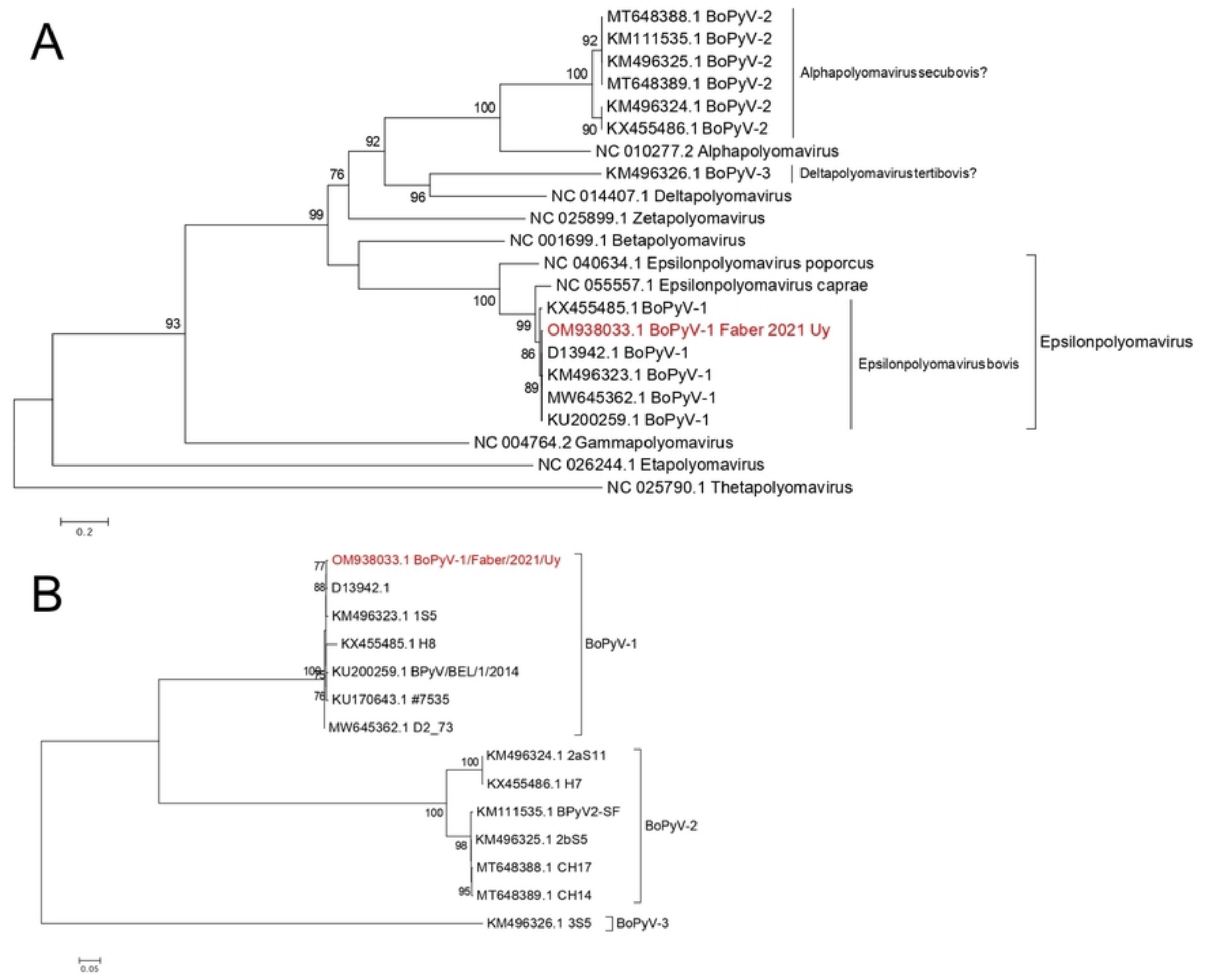
A
MT648388.1 BoPyV-2
KM111535.1 BoPyV-2
KM496325.1 BoPyV-2
MT648389.1 BoPyV-2
KM496324.1 BoPyV-2
KX455486.1 BoPyV-2
Alphapolyomavirus secubovis?
NC 010277.2 Alphapolyomavirus
KM496326.1 BoPyV-3
Deltapolyomavirus tertibovis?
NC 014407.1 Deltapolyomavirus
NC 025899.1 Zetapolyomavirus
NC 001699.1 Betapolyomavirus
NC 040634.1 Epsilonpolyomavirus poporcus
NC 055557.1 Epsilonpolyomavirus caprae
KX455485.1 BoPyV-1
OM938033.1 BoPyV-1 Faber 2021 Uy
D13942.1 BoPyV-1
KM496323.1 BoPyV-1
MW645362.1 BoPyV-1
KU200259.1 BoPyV-1
Epsilonpolyomavirus bovis
Epsilonpolyomavirus
NC 004764.2 Gammapolyomavirus
NC 026244.1 Etapolyomavirus
NC 025790.1 Thetapolyomavirus
0.2
B
OM938033.1 BoPyV-1/Faber/2021/Uy
D13942.1
KM496323.1 1S5
KX455485.1 H8
KU200259.1 BPyV/BEL/1/2014
KU170643.1 #7535
MW645362.1 D2_73
BoPyV-1
KM496324.1 2aS11
KX455486.1 H7
KM111535.1 BPyV2-SF
KM496325.1 2bS5
MT648388.1 CH17
MT648389.1 CH14
BoPyV-2
KM496326.1 3S5
BoPyV-3
0.05

Figure

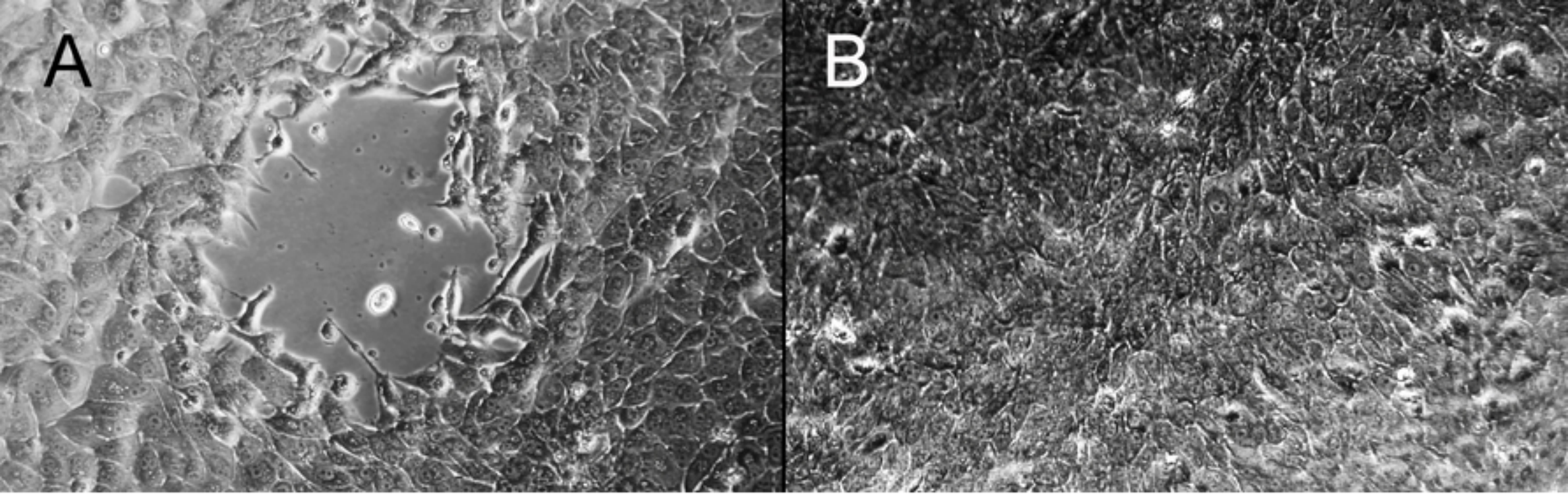

Figure

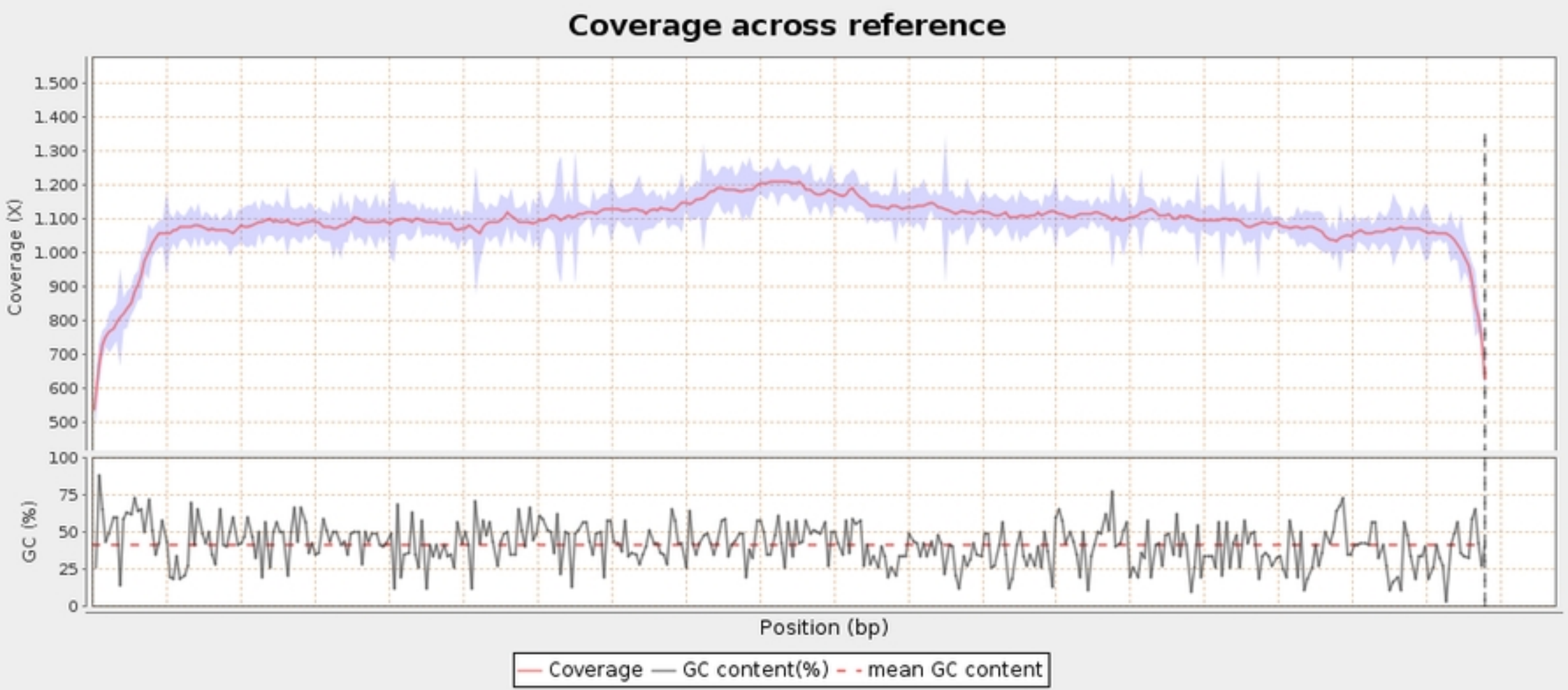
Coverage across reference
Coverage (X)
1.500
1.400
1.300
1.200
1.100
1.000
900
800
700
600
500
GC (%)
100
75
50
25
0
Position (bp)
Coverage
GC content(%)
mean GC content

Figure

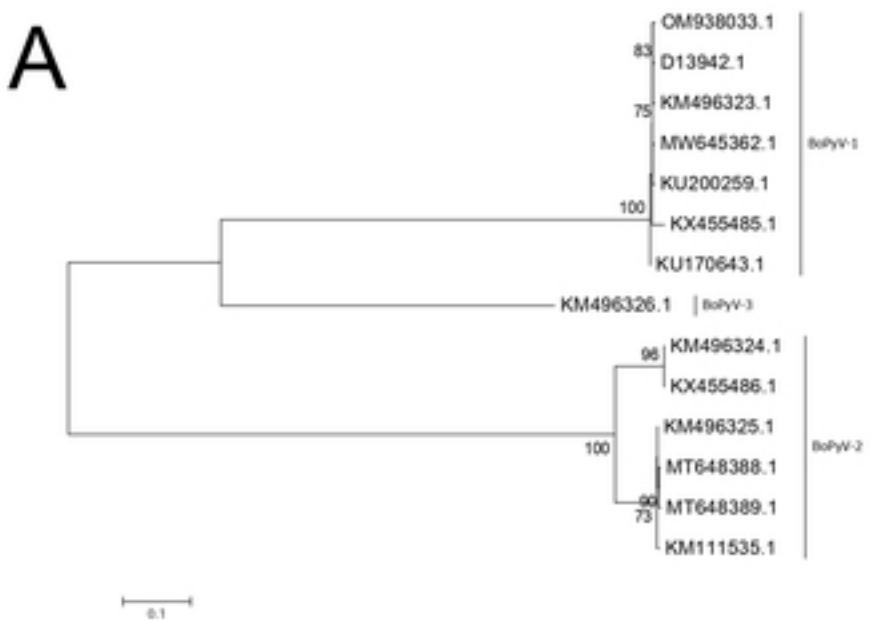

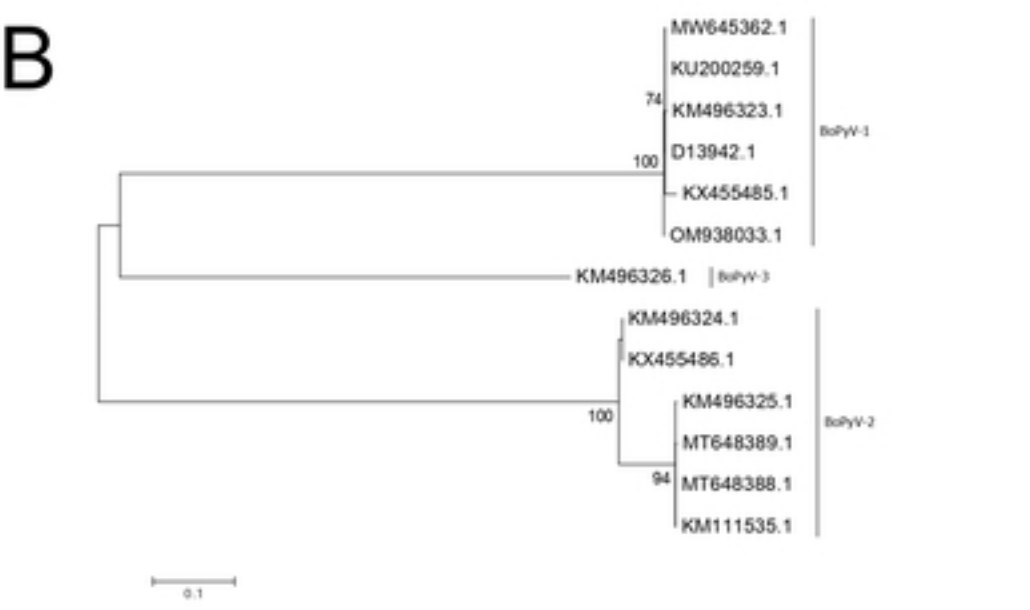

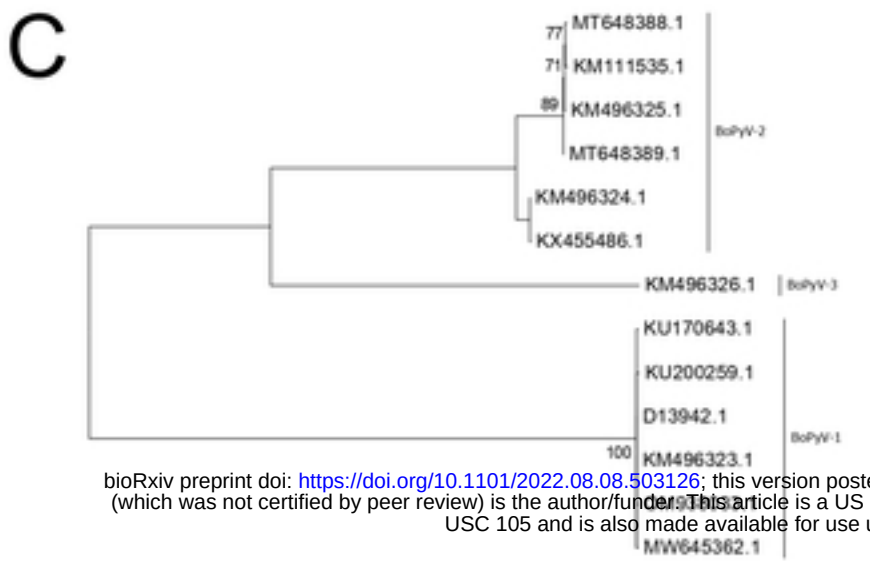

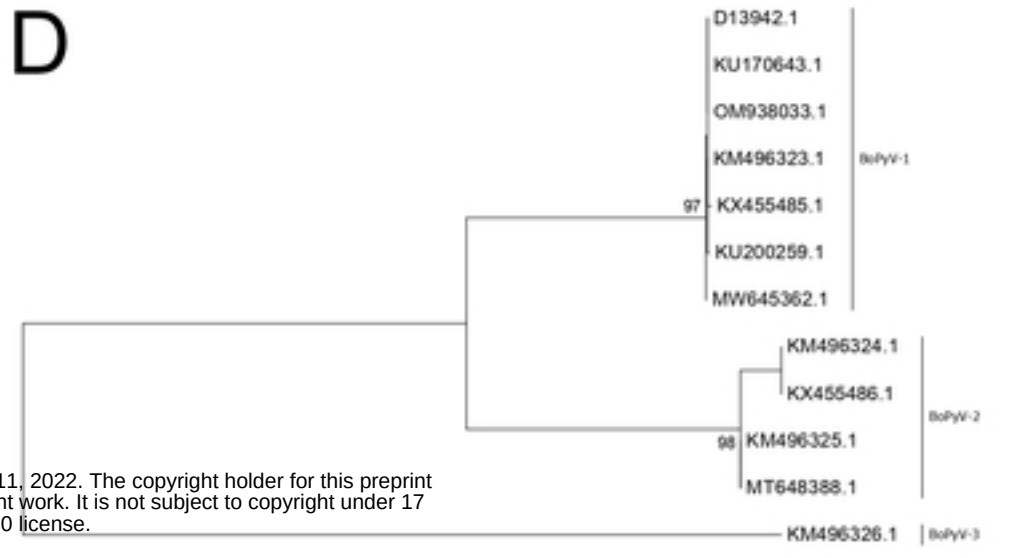

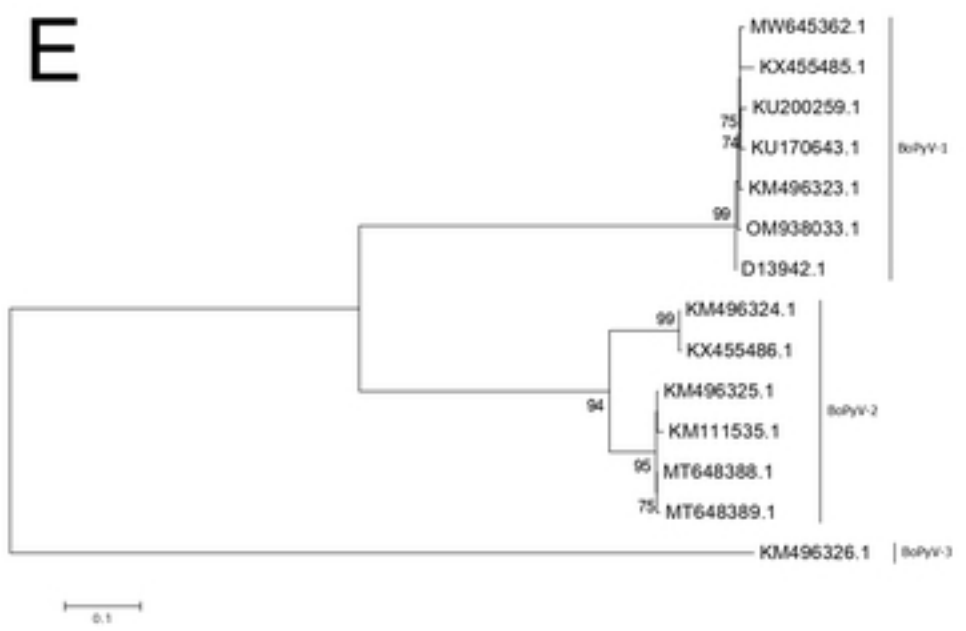

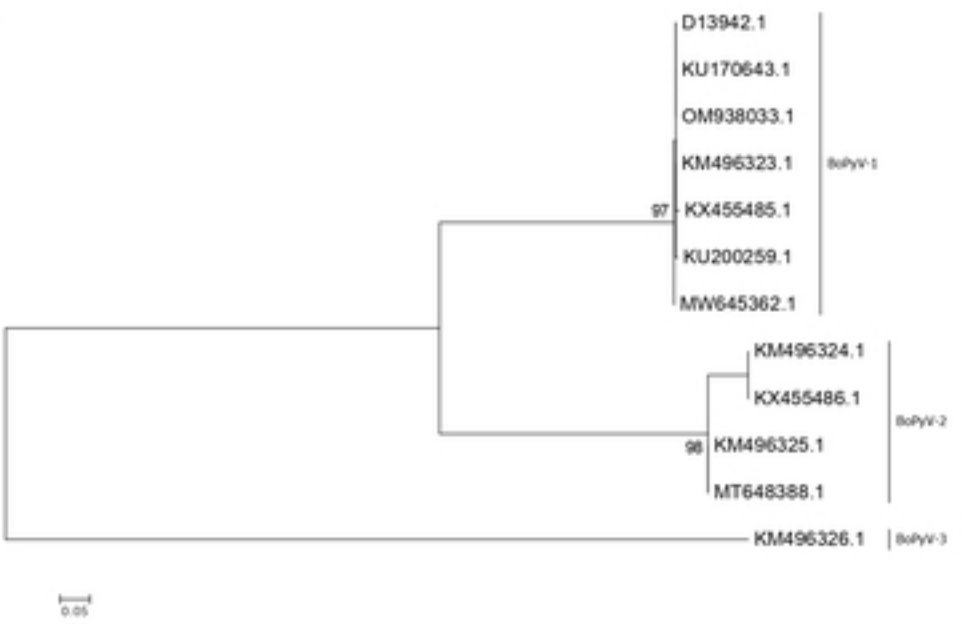

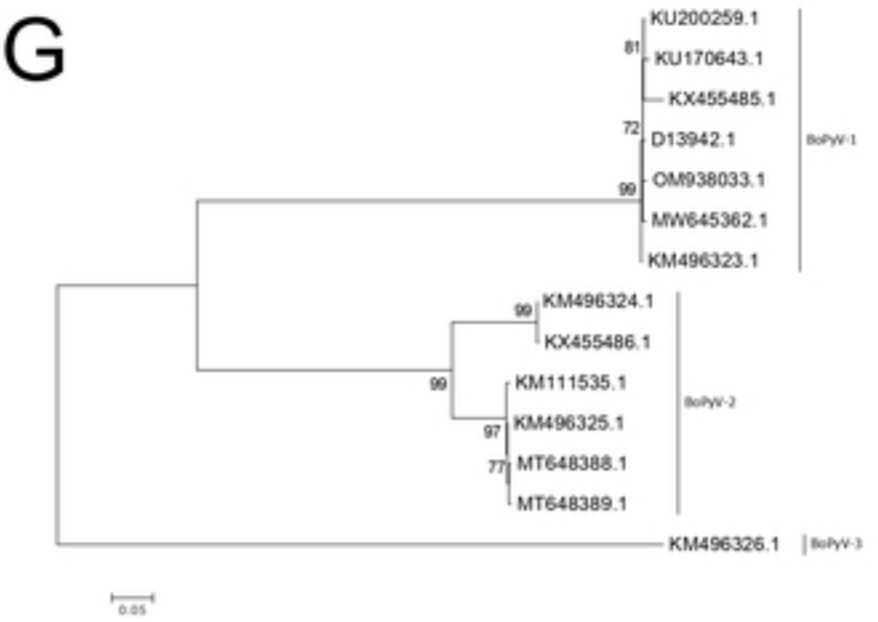

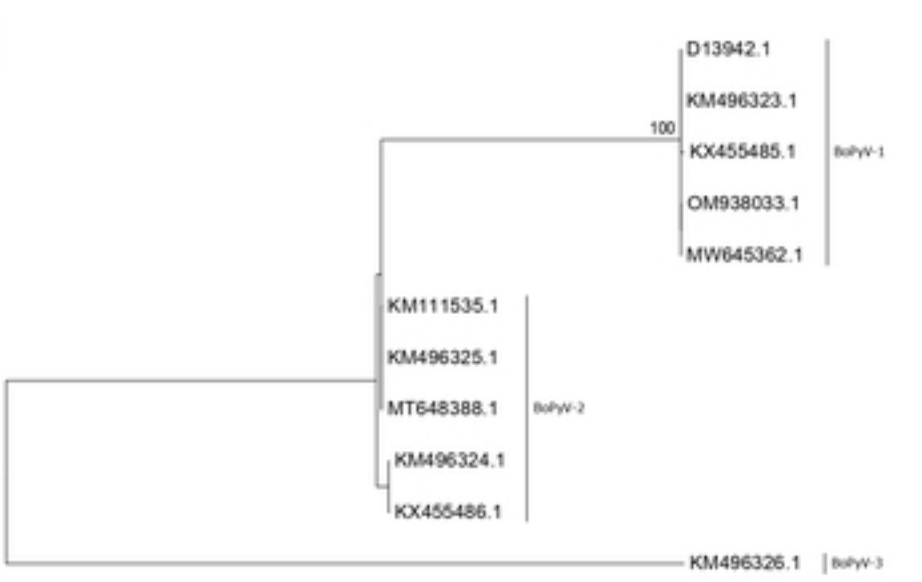

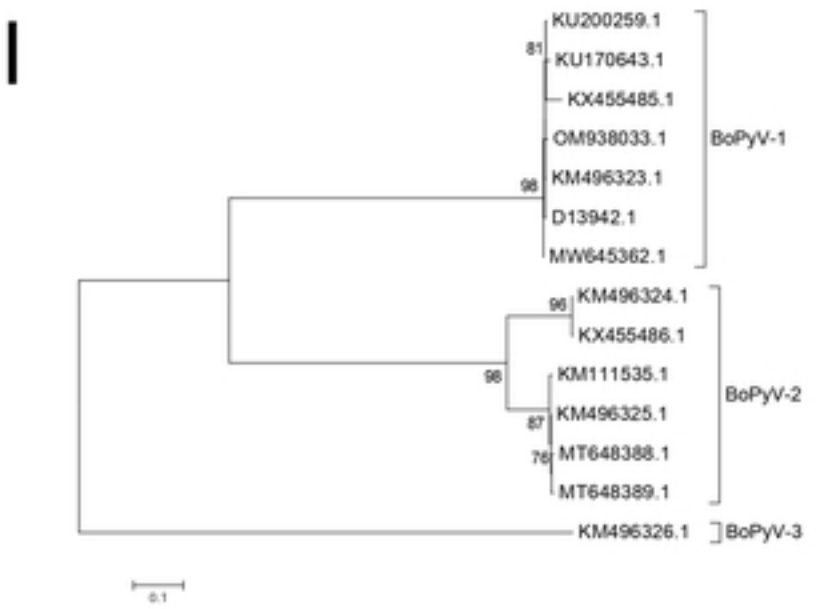

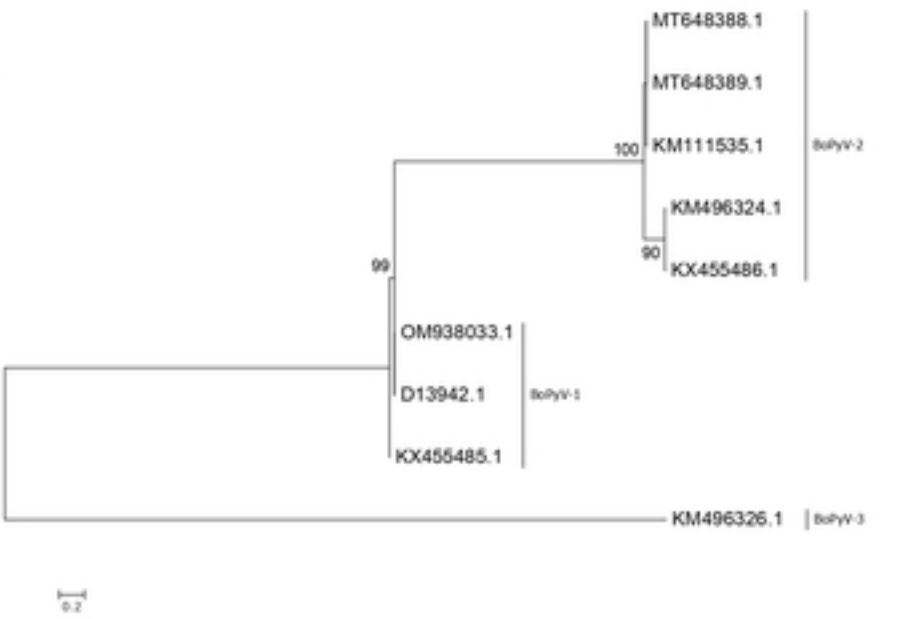

Figure